INDUCED MIXING IN A THERMALLY STRATIFIED FLUID

BY

HOMA JESSE LEE

SB, Massachusetts Institute of Technology
(1965)

Submitted in partial fulfillment

of the requirements for the degrees of

Civil Engineer

Master of Science

at the

Massachusetts Institute of Technology

(May 1968)

Signature of Author . . . .
Department of Civil Engineering, (May 1968)

Certified by. . . . . .
Thesis Supervisor

Accepted by . . . .
Chairman, Departmental Committee on Graduate Students

ABSTRACT

INDUCED MIXING IN A THERMALLY STRATIFIED FLUID

by

HOMA JESSE LEE

Submitted to the Department of Civil Engineering on May 24, 1968, in partial fulfillment of the requirements for the degrees of Civil Engineer and Master of Science.

Previous studies have shown that artificial mixing of thermally stratified lakes and reservoirs results in an improvement of their water quality. This investigation was undertaken to study various aspects of this process.

A large, circular water tank with a variable effective depth was used as a reservoir model. Thermal stratification was produced by radiation received from lamps suspended over the model. Mixing was induced by injecting nitrogen through a nozzle at the bottom center of the tank. Temperature measurements were made and the potential energy of the body of water was calculated at numerous times throughout each experiment.

Twelve experiments were made, in which the rate of gas injection, effective depth, and radiation being received during injection were varied. The behavior of the body of water under different radiation conditions without gas injection was studied so that a realistic estimate of efficiency and per cent of mixing could be made.

The per cent of mixing was shown to be linearly related to the logarithm of time with a constant of proportionality which was essentially the same for all experiments. The efficiency of mixing was shown to have little variance with gas injection rate, and it was suggested that the time of mixing was more pertinent to the engineer than efficiency. The product of injection rate and time of fifty per cent mixed was shown to be almost constant for a particular effective depth.

The data from several field tests was studied and a scheme for relating field and laboratory test results was proposed.

Thesis Supervisor: Donald R.F. Harleman

Title: Professor of Civil Engineering

ACKNOWLEDGMENT

The author wishes to thank Professor Donald R.F. Harleman for the personal interest and valuable suggestions which he extended during the course of this program.

TABLE OF CONTENTS

I. INTRODUCTION

Between the periods of mixing that take place in the spring and autumn, the phenomenon of thermal stratification often occurs in lakes and reservoirs. This results in the formation of horizontal layers of warm, relatively light water near the surface above colder, relatively heavy water. In terms of energy, this configuration is more stable than that of a non-stratified reservoir and, therefore, vertical motions, which would increase the energy of the system, are effectively damped. Decaying matter in the lower strata of the reservoir rapidly consumes the available dissolved oxygen. The water of these lower levels is prohibited by the stratification from moving to the surface to renew its oxygen supply, and only a small amount of oxygen will diffuse downward from the upper layers. The decay progresses to the anaerobic state, hydrogen sulfide and other unfavorable substances are produced, and the growth of certain algae is greatly accelerated.

These adverse results may prove fatal to many of the fish in both the reservoir and the downstream river (if the outlet works draw from the lower strata). Likewise, the feasibility of using the reservoir and river water for water supply is greatly reduced; the sulfide-laden water may corrode turbines, and the presence of algae and hydrogen sulfide may make the reservoir unsightly and odorous.

In recent years, several attempts have been made to reduce the stratification in reservoirs. In most of the early efforts, pumping of water from one depth to another was used with only qualified success. In 1956, Riddick [8] used a floating aerator to circulate the water of a small reservoir in New York. Since the air was released only eight feet below the surface, he was only partially successful in improving its water quality. Various other attempts followed, in which air jets and a device known as the Aero-Hydraulics Gun were used to mix small reservoirs [6]. The results were generally favorable. During 1964, 1965, and 1966, field tests were run by the Federal Water Pollution Control Administration in which mixing was induced by discharging bottom water at the surface using axial pumps, and in 1966 by discharging compressed air at the bottom [7,9,10,11]. In all cases destratification was achieved and most of the water quality parameters showed an improvement. Several of these field tests will be considered qualitatively later.

Several laboratory studies involving induced mixing in stratified bodies of water have also been conducted at the Massachusetts Institute of Technology. In 1961 Farmer, Franklin, and Wheeler studied forced convections in a rectangular tank of salinity-stratified water using water jets [3]. Gay and Hagedorn studied the same problem in 1962 using air injection [4]. In 1966, Brainard performed a series of tests on a large, circular, thermally-stratified tank of water in which mixing was induced by injecting gas at the bottom center of the tank [1]. The experiments which will be presented here are a continuation of the study begun by Brainard.

II. OBJECTIVES OF LABORATORY TESTING PROGRAM

Due to time and physical limitations, it is often difficult to run a series of field tests in which the effect of various parameters may be determined. One of the primary objectives of this experimental program, therefore, was to detect qualitative trends under controlled conditions which might not be as apparent in the field. These included the effects of variable gas injection rates, reservoir depth, and solar radiation received during the mixing process. A second objective was to attempt to correlate quantitatively the laboratory results with field results. In this way, future field behavior might be predicted and field performance improved.

III. APPARATUS

A. The Model

1. The Tank: The reservoir model consisted of a circular wooden tank approximately six feet in diameter, 2 1/2 feet deep, and with walls 1 3/4 inches thick. A 1/2 inch thick, marine plywood, false bottom was placed in the tank so that a relatively shallow effective water depth of 15 or 22 centimeters could be maintained, and at the same time the free surface could be kept a few inches below the rim of the tank near the heating apparatus suspended above.

2. Heating Apparatus: Thermal stratification was produced in the reservoir by two sets of lamps suspended at a height of 57 cm above the water surface. The height was chosen so as to provide essentially uniform radiation at a reasonable intensity. Dake used this apparatus in an earlier study and describes the lamps as follows [2]:

> "The surface of the water in the tank was heated by two sets of lamps manufactured by the Westinghouse Electric Corporation.
>
> Set 1. 13,400 watts H33-1-HS mercury vapor lamps and 4,250 watts H37-5kB mercury vapor lamps.
>
> Set 2. 12,250 watts R40/4 Infra-red lamps.
>
> The 400 watts, H33-1-HS mercury vapor lamps were the same type used by Askin and Willand (1960) in the Frankford Arsenal sun room design with the old designation L-H1-LG. A breakdown of the radiation spectrum gives a composition of 66.5 per cent infra-red (above 0.76), 25.2 per cent visible and 8.3 per cent ultra-violet (below 0.38). This compares with normal solar radiation composition of 50-55 per cent infra-red, 40-45 per cent visible and about 5 per cent ultra-violet. The spectrum of the R40/4 infra-red lamp ... contains about 90 per cent infra-red energy and the remainder visible...
>
> The spacing of the two sets of lamps is shown in the plan

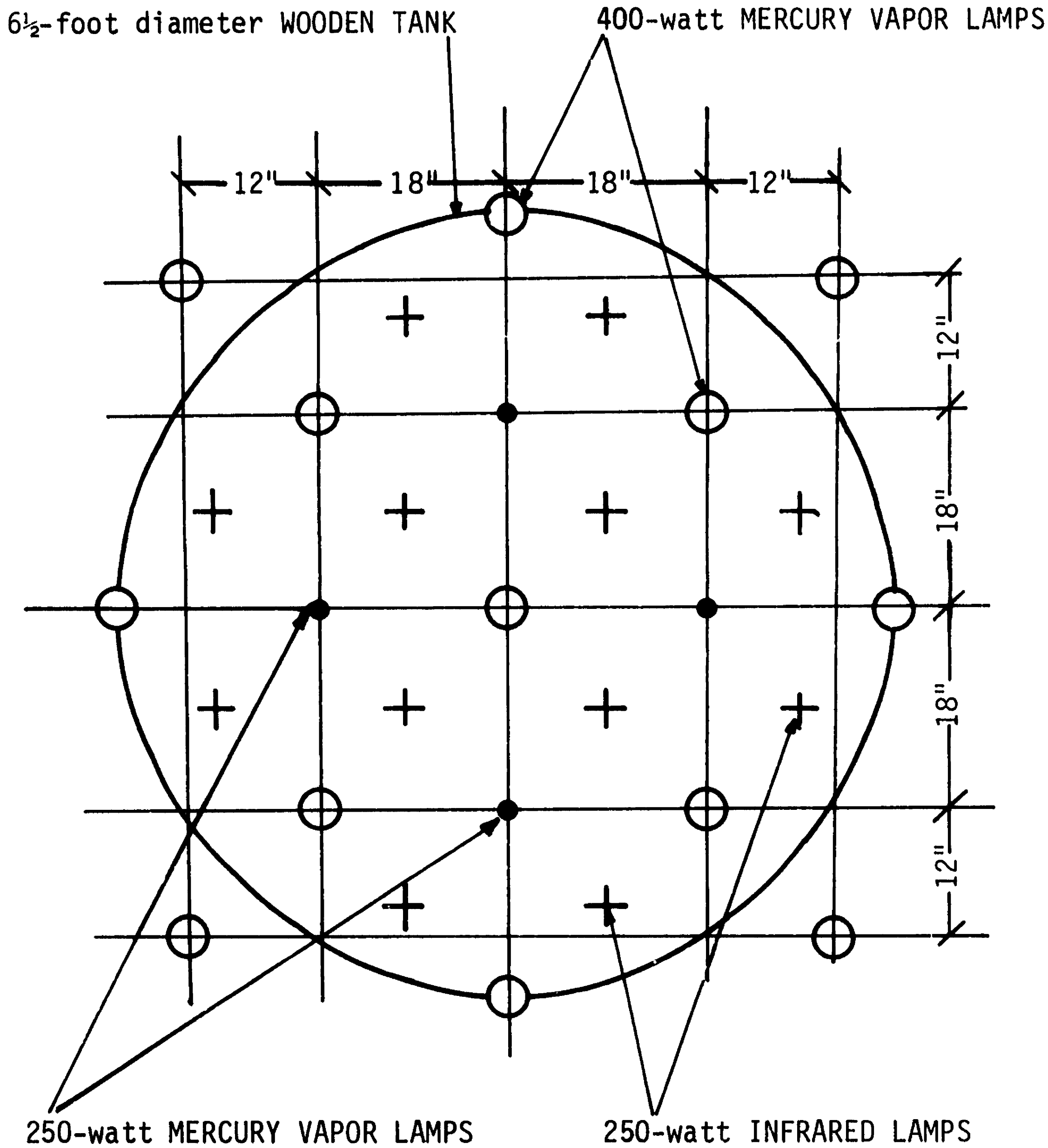

Fig. 1. Plan View of Lamp Arrangement

in figure 1 ... Vertical temperature profiles taken at random throughout the tank did not reveal any significant pattern of irregularity. Measurements of thermal stratification close to the tank wall were practically the same as those near the center, indicating no heat transfer through the walls ...

All lamps except H37-5KB had internal coating reflectors and external reflectors were provided for the H37-5KB lamps. The mercury vapor lamps were fed from the hydrodynamic laboratory mains through ballasts specified by the manufacturers. The vertical position of the lamps could be changed relative to a fixed water surface by moving up or down their horizontal supporting beams along four vertical columns erected symmetrically over the circular tank."

3. Mixing Apparatus: Mixing of the thermally stratified body of water was achieved by injecting nitrogen through a nozzle located at the center of the false bottom. The nozzle consisted of a 3/4 inch long, 6 mm O.D., .25 mm I.D. segment of Pyrex capillary tubing inserted into a section of 1/8 inch flexible plastic tubing which extended through an opening in the false bottom. The nozzle assembly projected 2.65 cm above the false bottom. The tubing was in turn connected to a water collection container with a drain for drawing off water which might collect in the lines between runs.

The gas source was a tank of nitrogen compressed under approximately 2500 psi. Flow was regulated by a Parox type R-2052 two-stage pressure regulator and a needle valve. The regulator provided approximately the necessary head loss required, with the needle valve furnishing the final adjustment. After the flow passed the needle valve it was monitored by a Fisher and Porter flowrator type M3-1288/1 flow meter. The pressure relative to the atmosphere was measured by a water manometer placed in the line immediately after the flow meter. Flow proceeded from this point directly to the water collection container beneath the false bottom. A schematic diagram of the laboratory equipment is provided in Fig. 2.

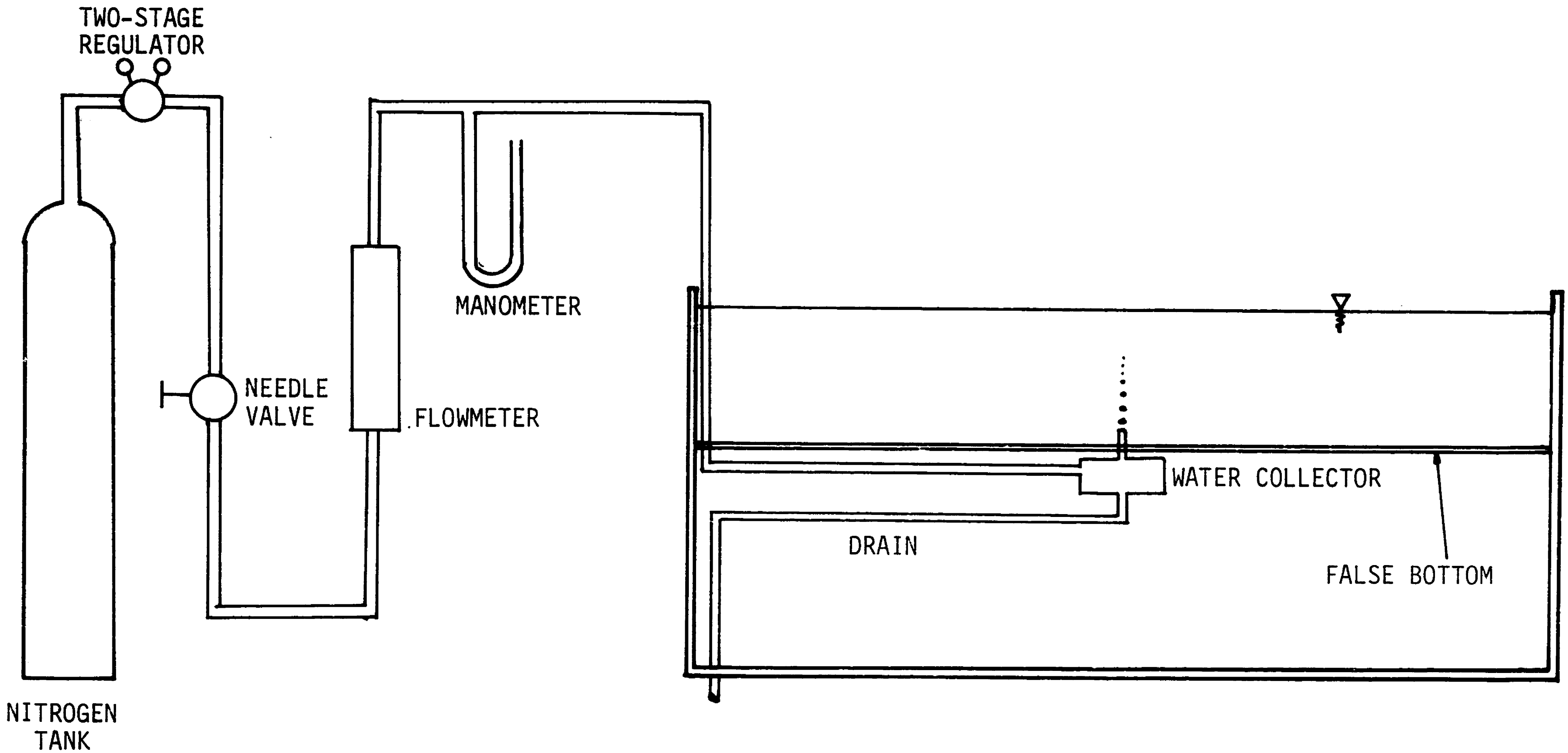

Fig. 2. Mixing Apparatus

B. Instrumentation

Temperature measurements were made with a motorized probe equipped with a Type GA 51P6 thermistor bead manufactured by Fenwal Electronics, Inc, Framingham, Massachusetts. The bead was imbedded in the top of a small glass probe which was mounted on a section of 0.25 inch O.D. plastic tubing. The tubing was in turn attached to a Lory Type A depth gage which could be raised or lowered with a small D.C. motor. By measuring the voltage drop across a potentiometer attached to the gears in the motor, it was possible to determine the relative elevation of the probe. Wires were run from the thermistor, up the center of the plastic tube, to an Amphenol type 126-198 socket. From here, connecting wires led to a precision Wheatstone bridge, the circuit for which is shown in Fig. 3. The probe assembly was calibrated in a constant temperature bath using a Kessler Co. Type M 1-5061 thermometer as a reference. The voltage unbalance of the bridge was measured with a Digitec model number 201 digital D.C. voltmeter. A calibration curve was constructed in which voltage unbalance was plotted versus temperature.

The motorized probe was mounted on a 9 foot long, 1/4 inch thick, 2 inch wide aluminum angle which was placed across the tank and which could be rotated about one end. By rotating this device, the probe could be moved to pratically any radial distance from the center. Photographs of the probe and of the mounting scheme are shown in Figs. 4 and 5.

In order to measure a temperature profile at a particular location and time, the thermistor was raised from the effective bottom of the tank

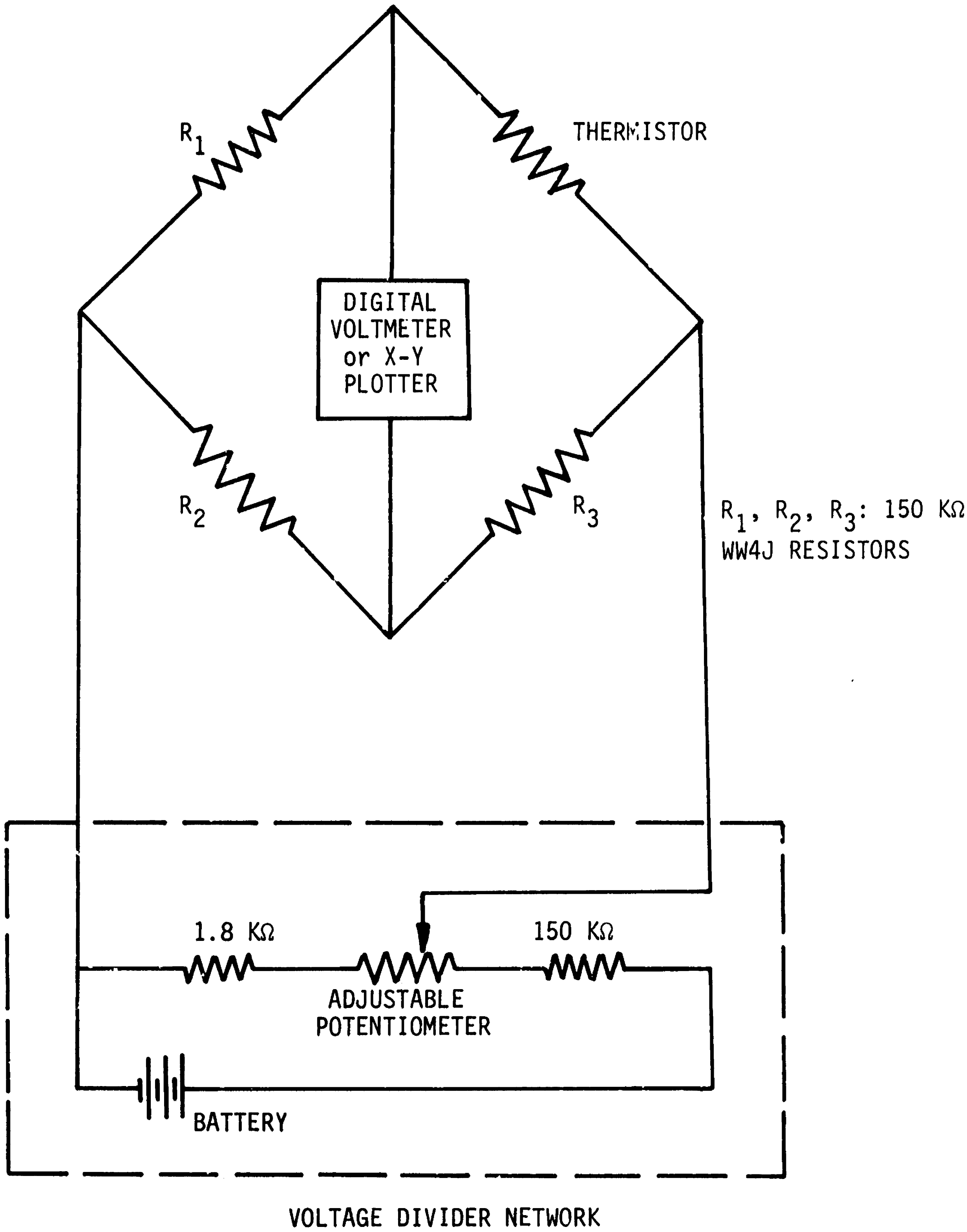

Fig. 3. Bridge Circuit

to the surface. For the first nine runs presented here, the voltage drop across the motor potentiometer was plotted on the vertical axis and the voltage unbalance across the bridge was plotted on the horizontal axis of a Bolt, Beranek, and Newman Model number 800A Plotamatic X-Y plotter. For the last three runs, these two voltages were measured by digital voltmeters and were plotted manually. Photographs of the apparatus for each of these schemes are presented in Figs. 6 and 7. These voltage plots were converted into temperature-elevation plots using the thermistor and vertical deviation calibration curves.

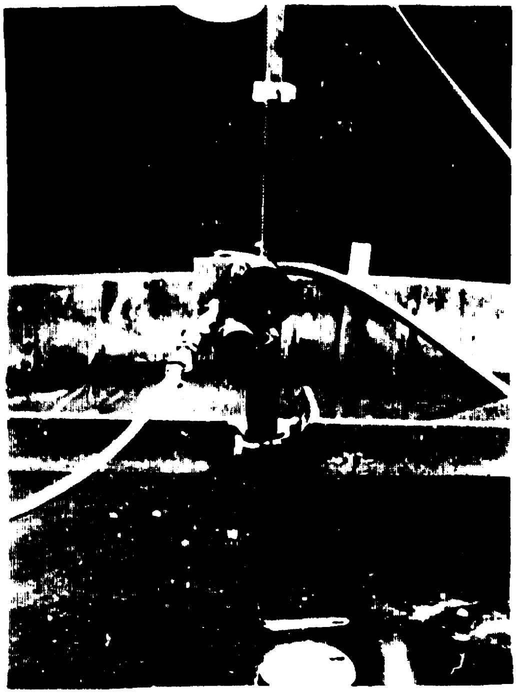

Fig. 4. Motorized Thermistor Probe

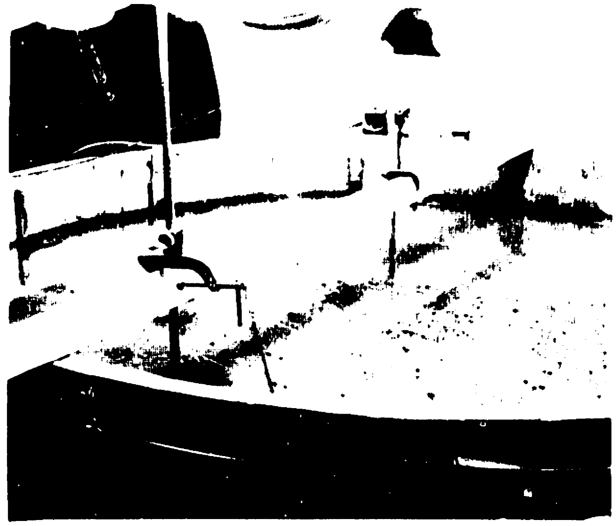

Fig. 5. Probe Mounting Scheme

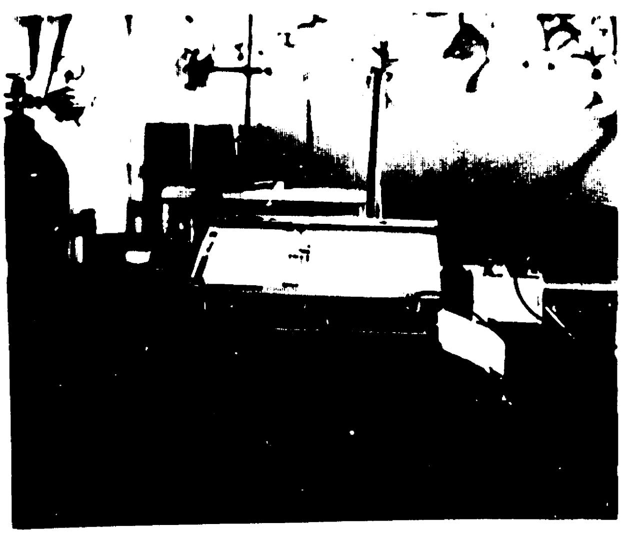

Fig. 6. Apparatus for Automatic Plotting

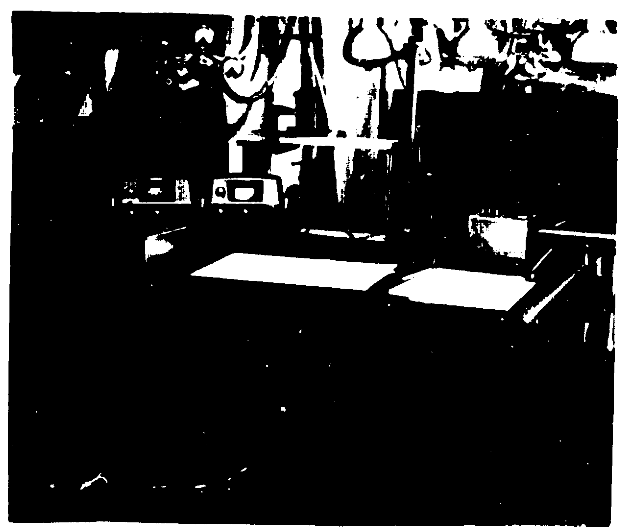

Fig. 7. Apparatus for Manual Plotting

IV. PROCEDURE

Before each run was begun, the water level was checked with the aid of a point gage mounted on the aluminum angle, and additional water was added to provide the appropriate depth. The water was thoroughly mixed by hand and allowed to come to rest. The gas lines were cleared of water, and an initial temperature profile was made to determine the thoroughness of the mixing and the initial water temperature.

The lamps were turned on at this point and allowed to heat the water for a particular length of time. In most of the runs gas injection was begun either some period of time before or immediately after the lights were turned off. This injection consisted of applying about 5 psi of nitrogen to the gas line by adjustment of the two-stage regulator and then of adjusting the needle valve to obtain the desired flow rate.

Temperature measurements were made at several times during each run. Preliminary tests showed that there was little radial variation in temperature distribution when gas was not being injected. For these cases, the probe was set at a radial distance of 19 inches from the injection nozzle and raised by the motor at a velocity of about 1.5 feet/minute. The resulting voltage plot was taken to be representative of the entire tank. About 45 seconds were required for each of these profiles.

When gas was being injected at the time of measurement, radial variation of the temperature profile was great enough to warrant measurement of the temperature distribution at several locations. The probe was set at a radius of 9 inches and a traverse, such as described above, was made. The probe was then moved manually, by rotating the aluminum angel to first a radius of 19 inches and then a radius of 28 inches. Traverses were made at each point. The time required for this procedure was about 150 seconds. The resulting profiles were weighted according to the area over which each was assumed to be applicable and averaged in order to obtain one representative profile for the entire tank. The area of applicability for the first traverse was

$$\pi \left(\frac{19'' + 9''}{2} \right)^2 ;$$

for the second traverse,

$$\pi \left[\left(\frac{28'' + 19''}{2} \right)^2 - \left(\frac{19'' + 9''}{2} \right)^2 \right] ;$$

and for the third,

$$\pi \left[\left(\frac{37'' + 28''}{2} \right)^2 - \left(\frac{28'' + 19''}{2} \right)^2 \right] .$$

V. EXPERIMENTS

Twelve experiments were run in order to study the effects of induced mixing in a laboratory situation. Quantities which were varied included the effective depth of the laboratory lake, the rate of gas injection, the initial temperature profile, and the amount of radiation received during the gas injection. In four of these experiments, the behavior of the tank of stratified water without gas injection was studied. In this way the changes produced by gas injection in the other runs could be compared with the changes which would have occurred without injection. Table 1 summarizes the general characteristics of each experiment.

RUN NUMBER	DATE	DEPTH (cm)	TIME GAS INJECTION STARTED (minutes after lamps turned on)	TIME LAMPS TURNED OFF (minutes)	TIME OF LAST PROFILE (minutes)	GAS INJECTION RATE, Q (cc/minute)	BAROMETRIC PRESSURE (inches of mercury)	AIR TEMPERATURE (^oF)	FLOW METER PRESSURE (feet of water)	WATER TEMPERATURE BEFORE LAMPS TURNED ON (^oC)
1	3/26/68	22	-	510	510	-	-	74	-	18.7
2	3/30/68	22	240	240	418	175	29.92	80	.82	19.9
3	3/31/68	22	235	235	355	100	29.97	79	.75	20.75
4	4/1/68	22	207	207	327	250	29.90	77	.92	22.3
5	4/2/68	22	-	323	568	-	-	80.5	-	19.05
6	4/3/68	22	-	171	430	-	-	81	-	21.1
7	4/5/68	22	0	248	248	100	29.80	84	.93	22.1
8	4/7/68	22	195	465	465	100	30.12	77	.93	19.5
9	4/8/68	22	257	257	459	75	29.93	79	.82	24.0
10	4/10/68	15	-	186	306	-	-	81	-	19.3
11	4/11/68	15	190	190	285	250	30.19	79	.75	20.0
12	4/12/68	15	175	175	275	100	30.22	85	.67	20.25

Table 1

VI. RESULTS

A. Temperature Profiles

In Run 1, the lamps were left on for 510 minutes and the temperature distribution was measured at intervals of 15 to 30 minutes. Figure 8 shows several of these temperature profiles (y is the elevation above the false bottom, and t is the length of time after the lamps were turned on). As may be seen, most of the initial heating is near the surface, while most of the later heating occurs near the bottom. After the passage of about 200 minutes, the temperature differential between the surface and bottom reaches a maximum of about 18^{o} C and then begins to decline. Figure 9 shows typical temperature profiles for actual reservoirs during the summer months. As may be seen, the temperature differential between surface and bottom ranges from about 15 to 20^{o} C. Therefore, by leaving the lamps on for about 200 minutes, one obtains a reasonably good approximation of field stratification conditions. For most of the runs in which gas was being injected, the lamps were left on for about this period of time. In addition, temperature profiles were measured at several times during the heating phase to determine whether or not a satisfactory stratification pattern has developed.

Figures 10 through 20 show selected temperature profiles for runs 2 through 12 (t' is the time, in minutes, after either the lamps were turned off or gas injection was begun). For cases in which gas was being injected at the time of measurement, the temperature profile shown is the weighted average discussed in Section IV.

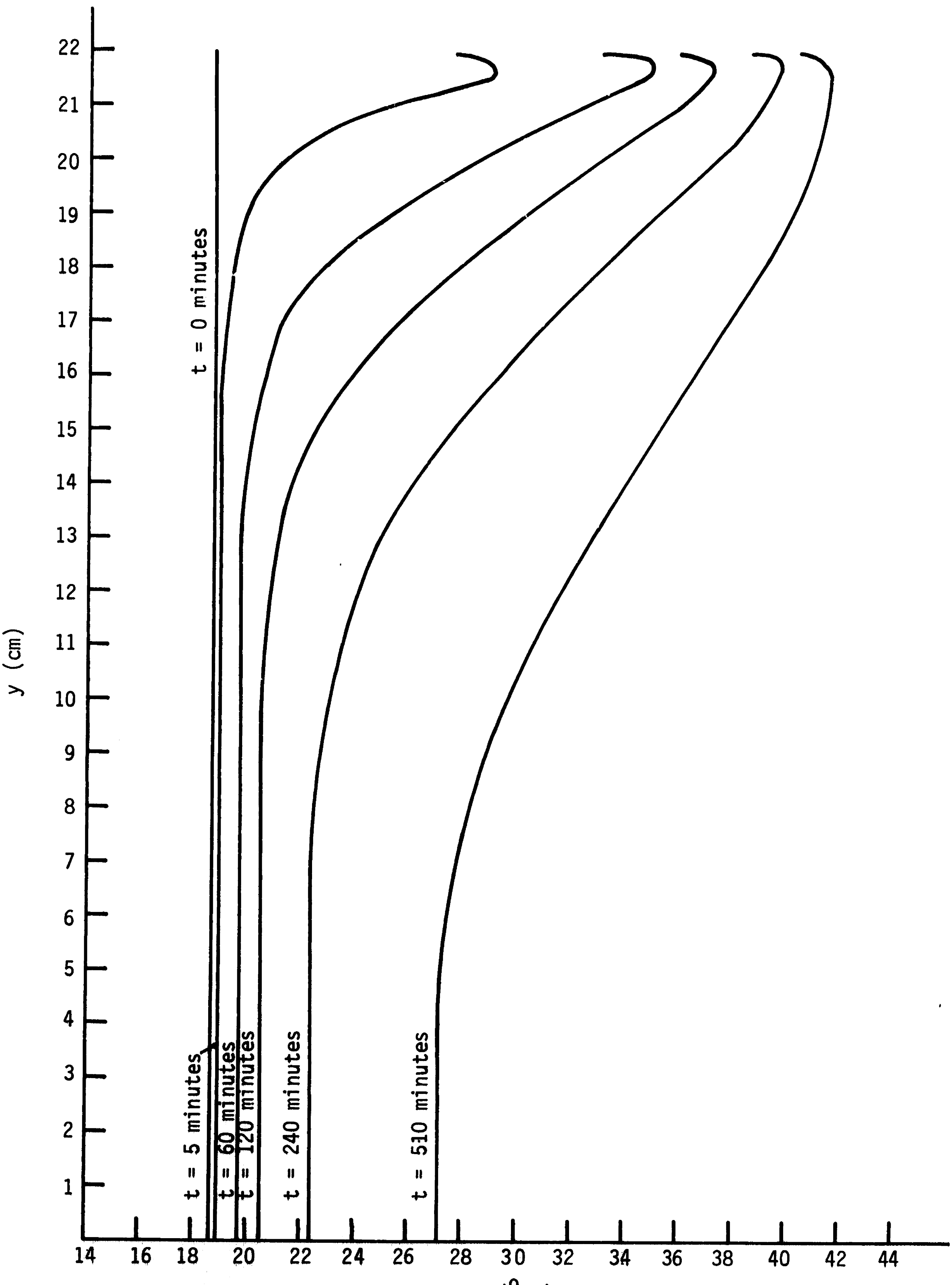

Fig. 8. Temperature Profiles for Run 1

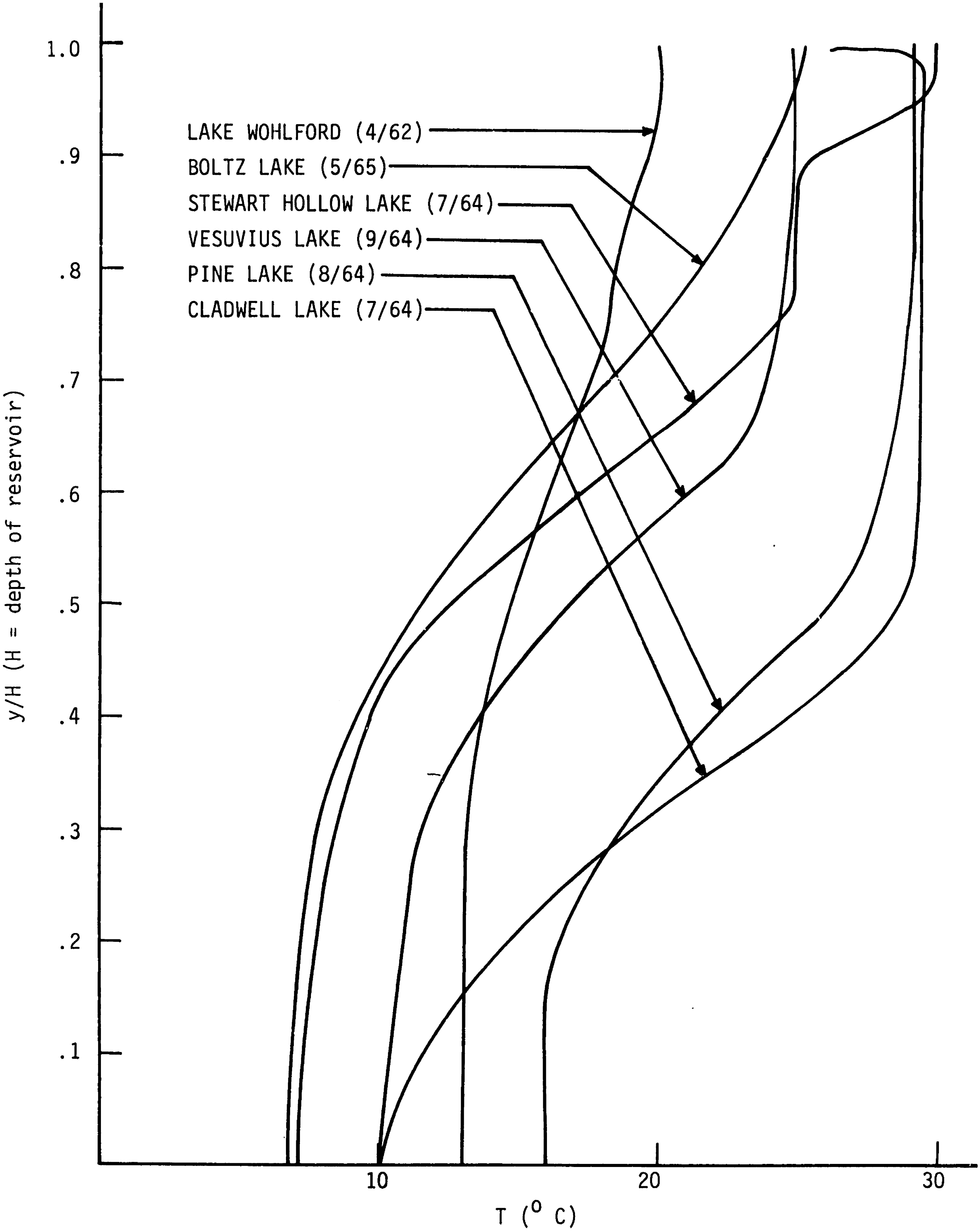

Fig. 9. Typical Summer Temperature Profiles in the Field

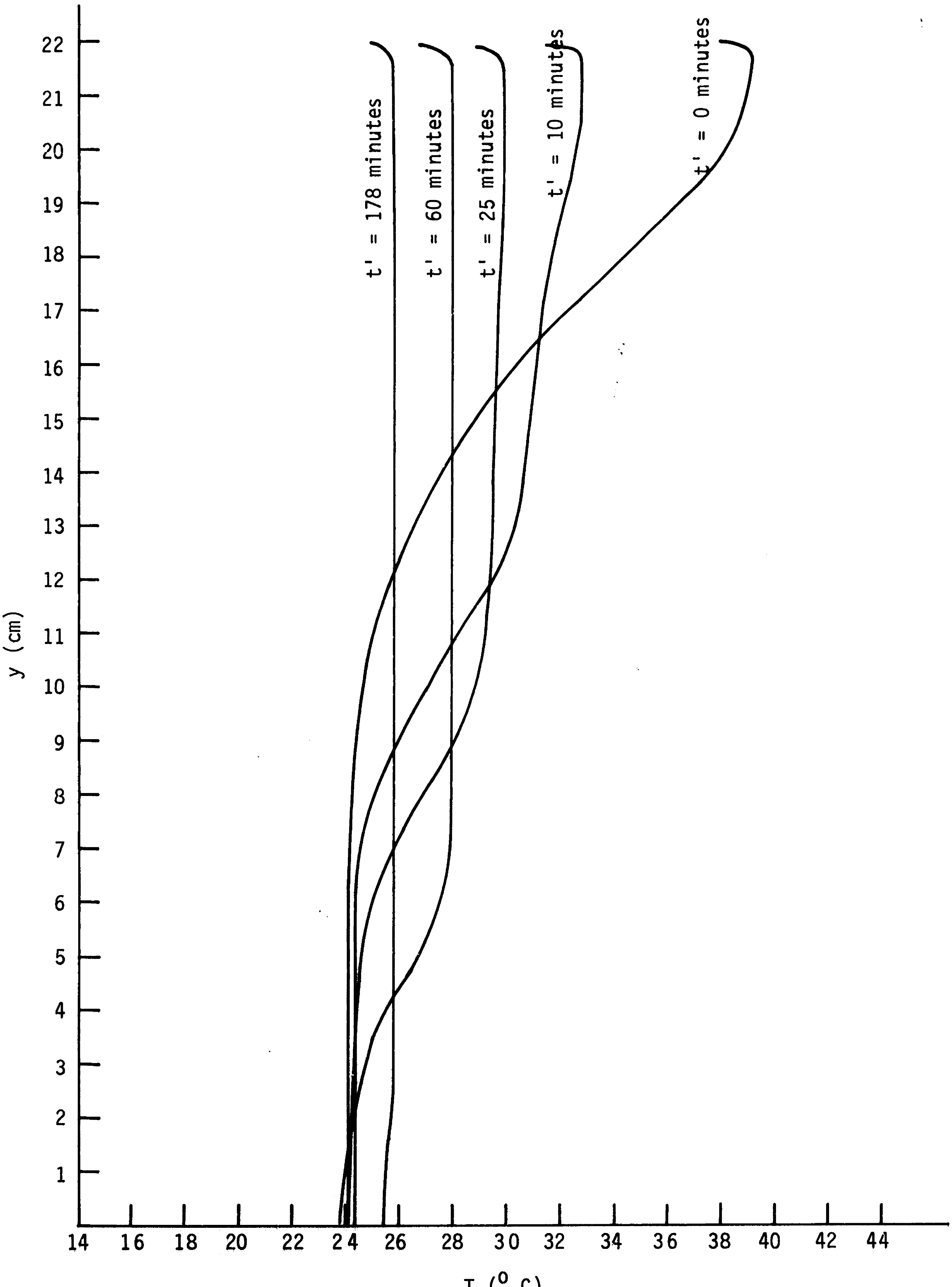

Fig. 10. Temperature Profiles for Run 2

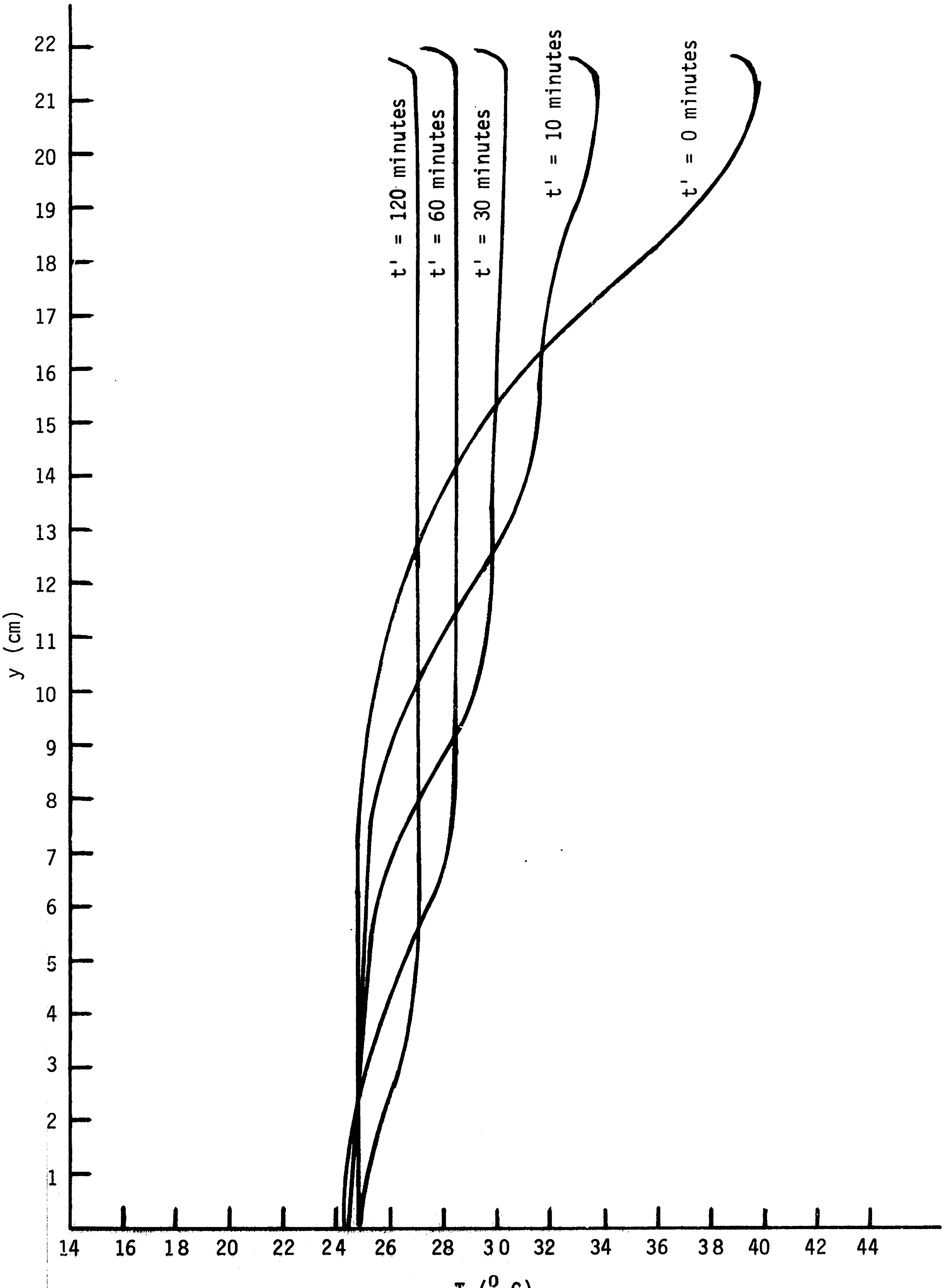

Fig. 11. Temperature Profiles for Run 3

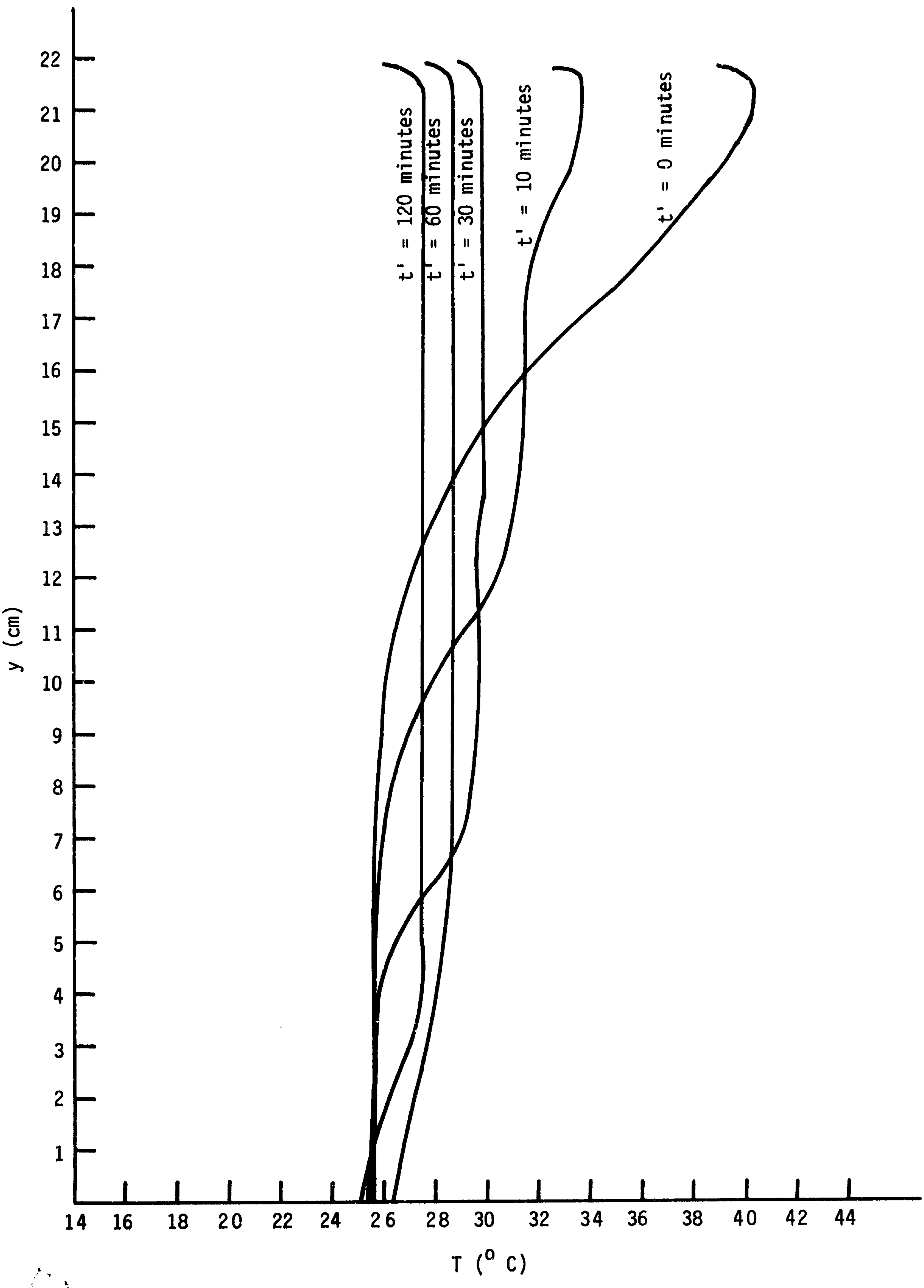

Fig. 12. Temperature Profiles for Run 4

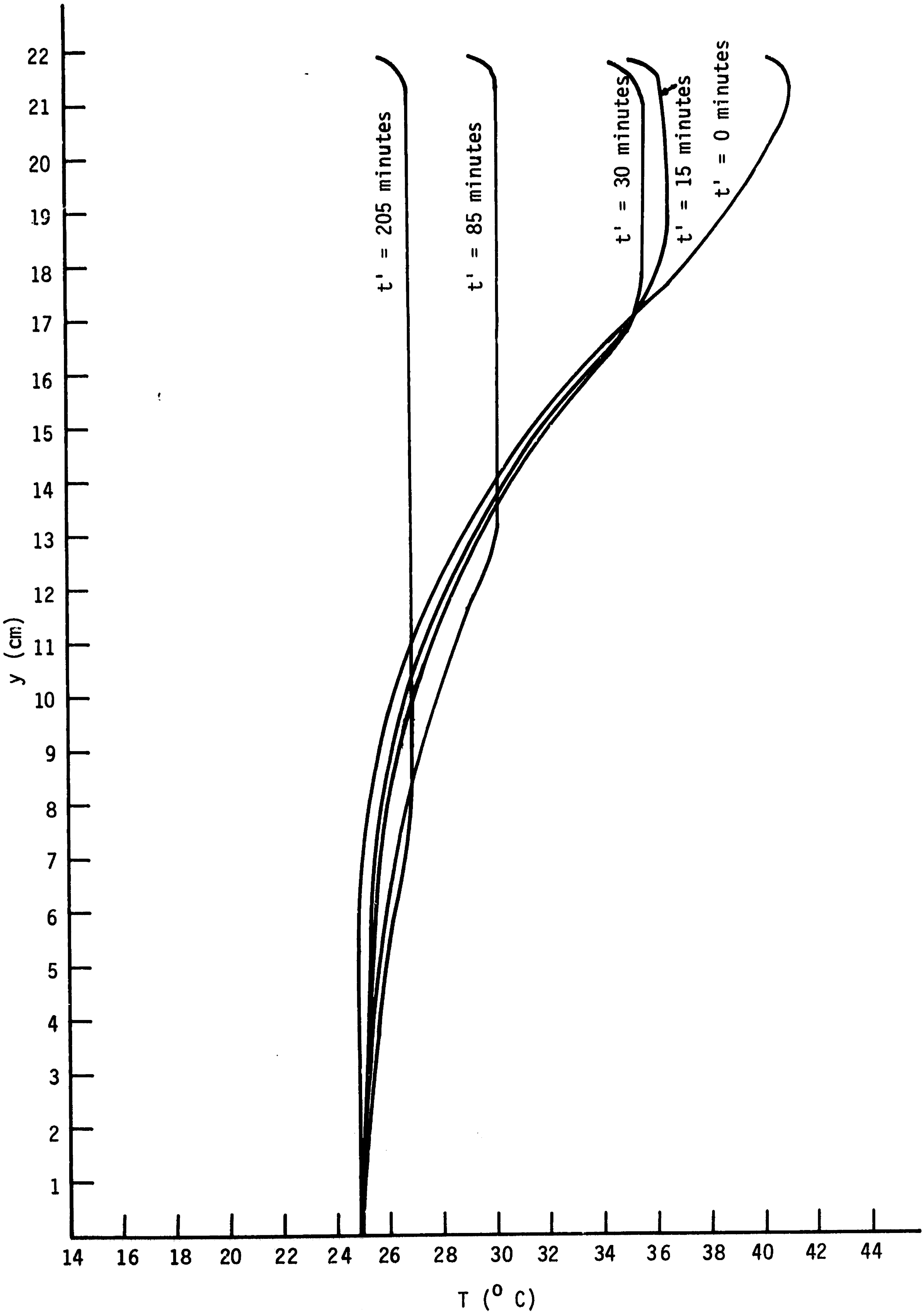

Fig. 13. Temperature Profiles for Run 5

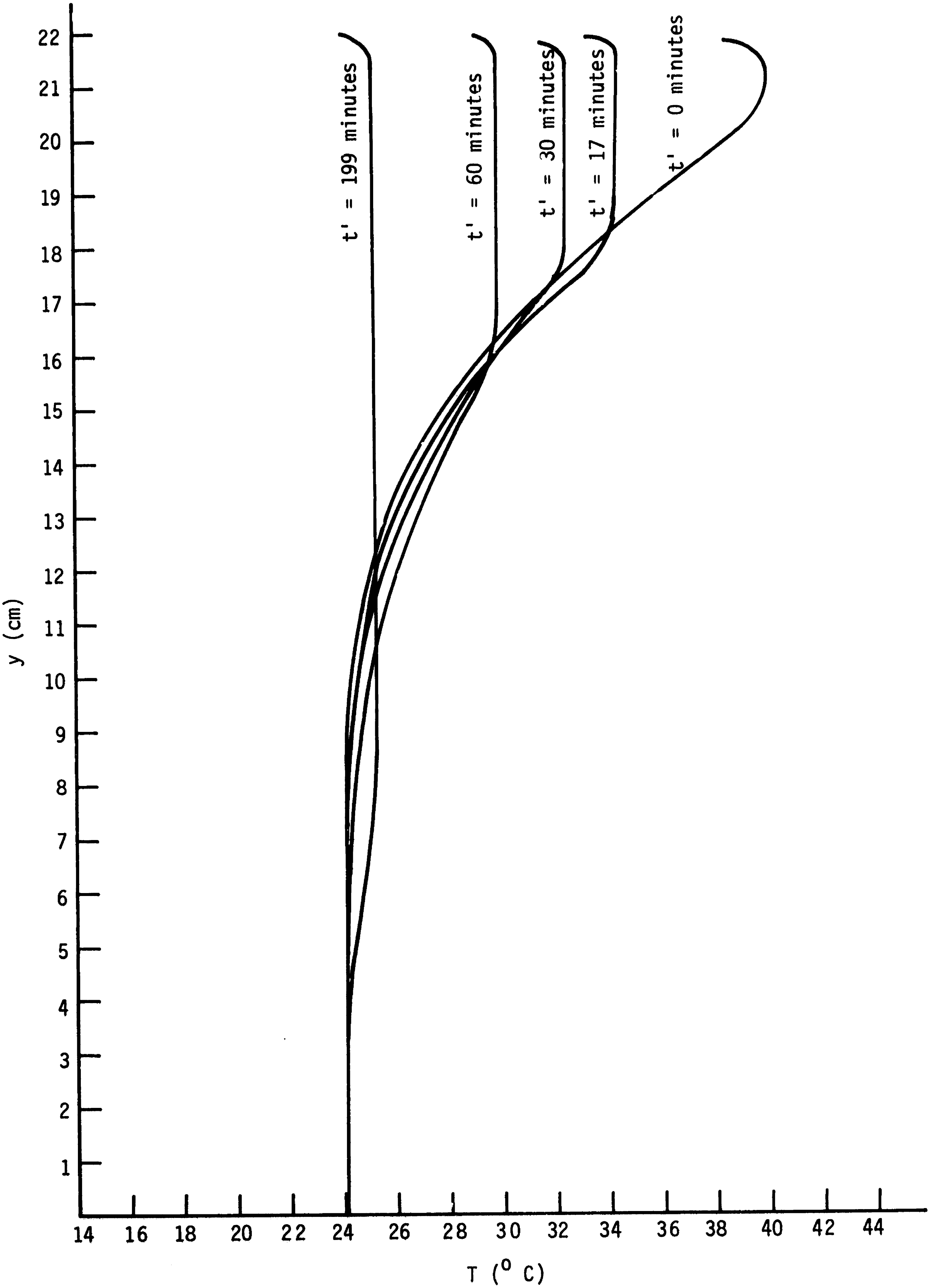

Fig. 14. Temperature Profiles for Run 6

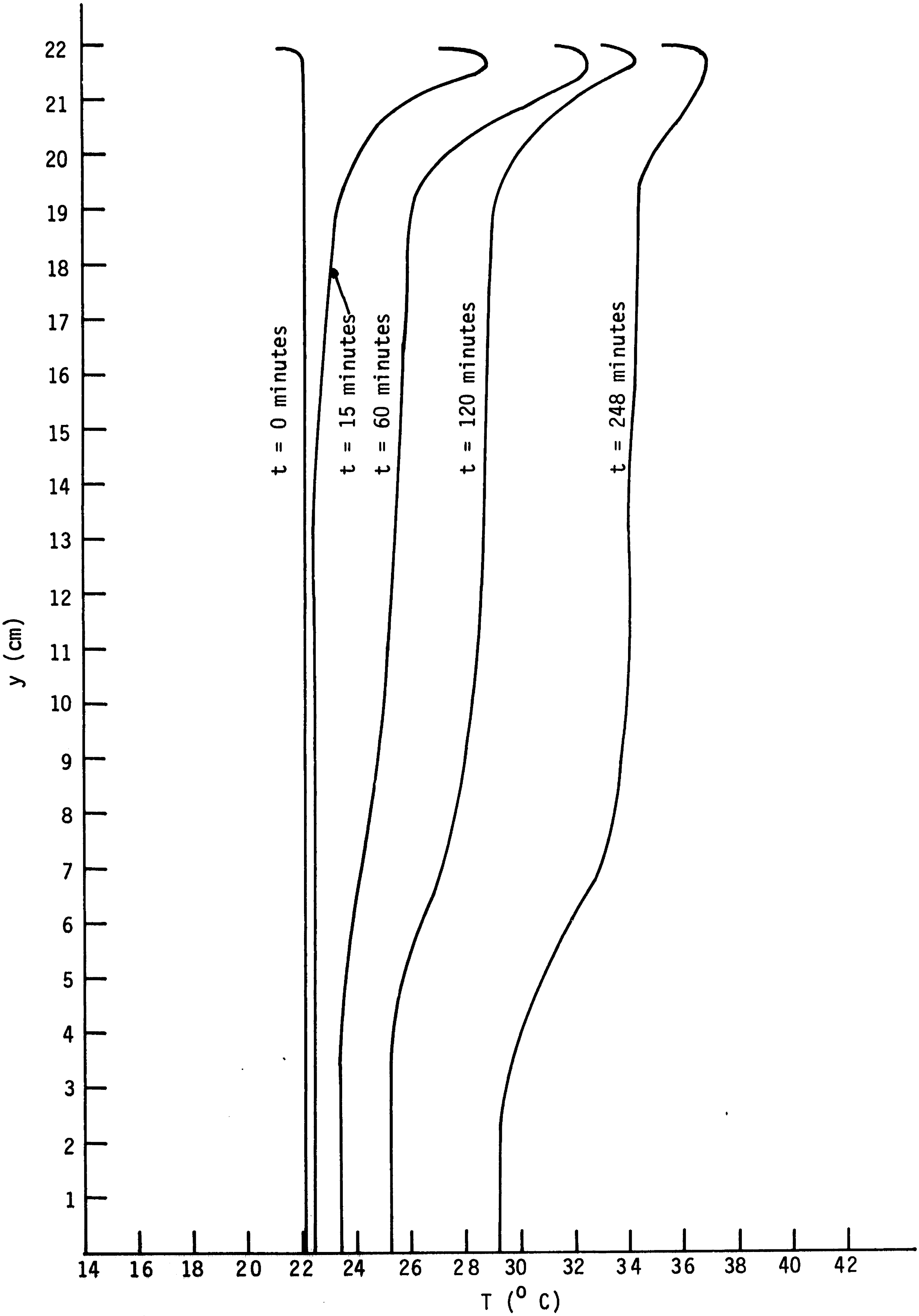

Fig. 15. Temperature Profiles for Run 7

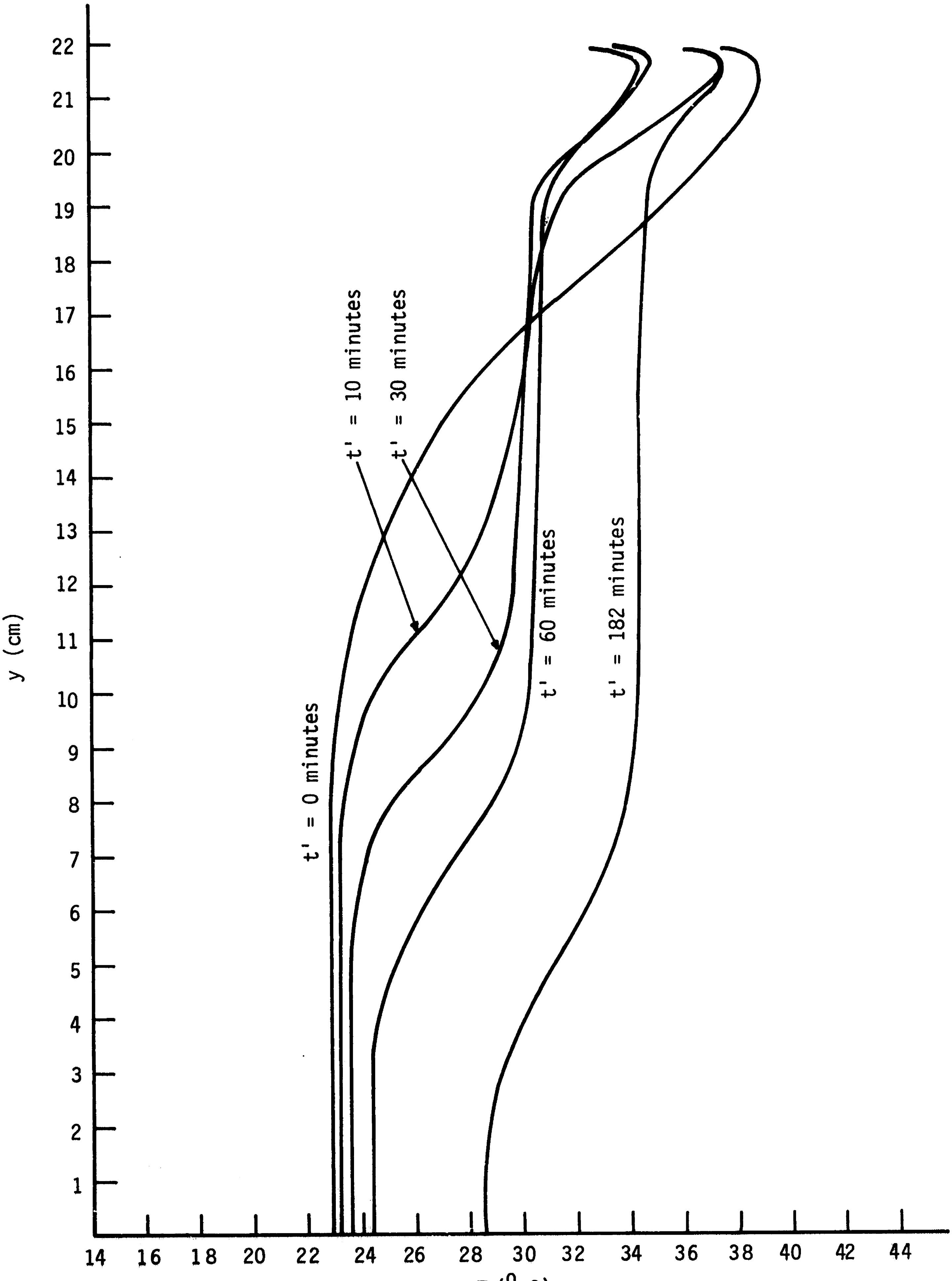

Fig. 16. Temperature Profiles for Run 8

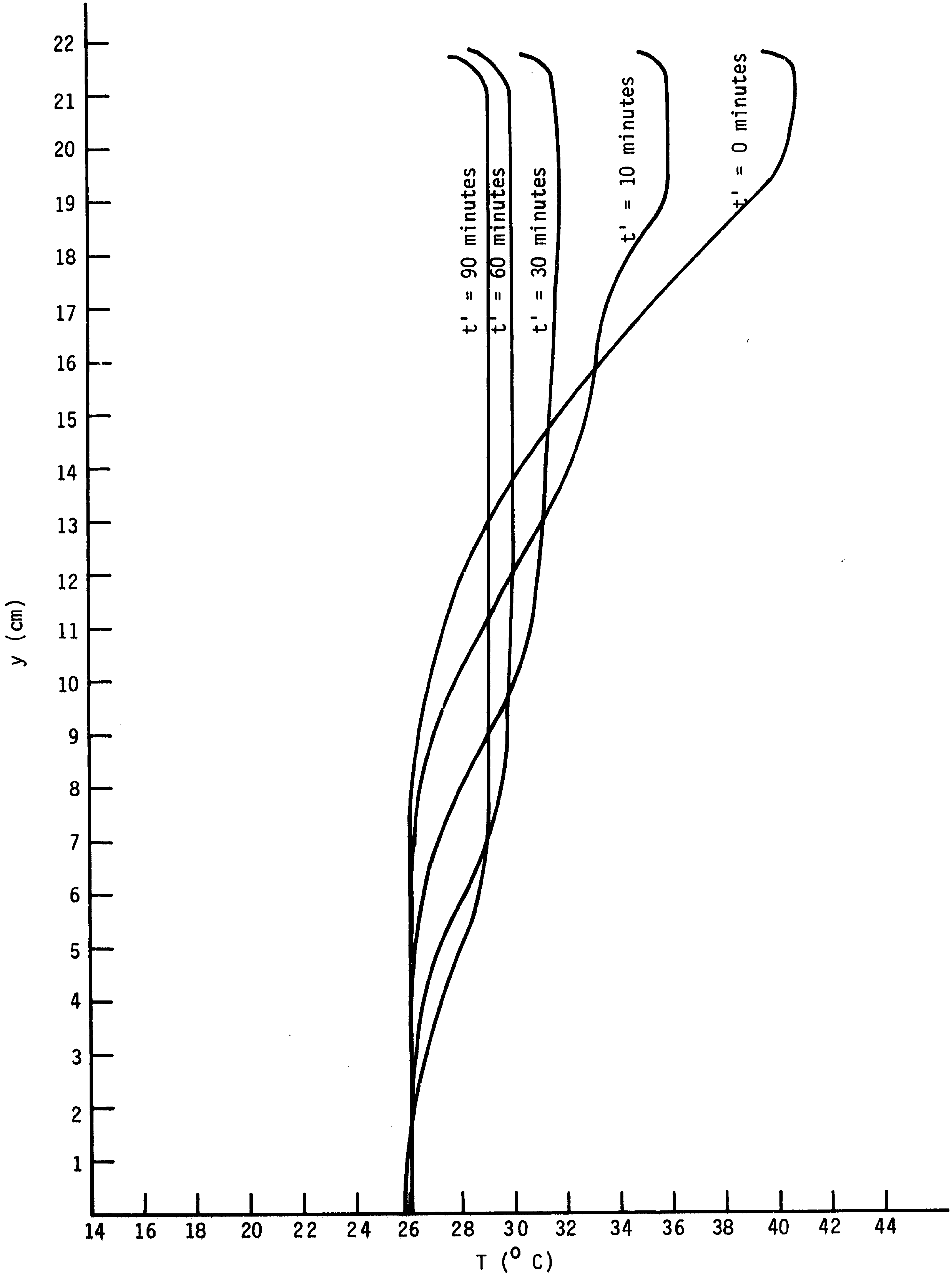

Fig. 17. Temperature Profiles for Run 9

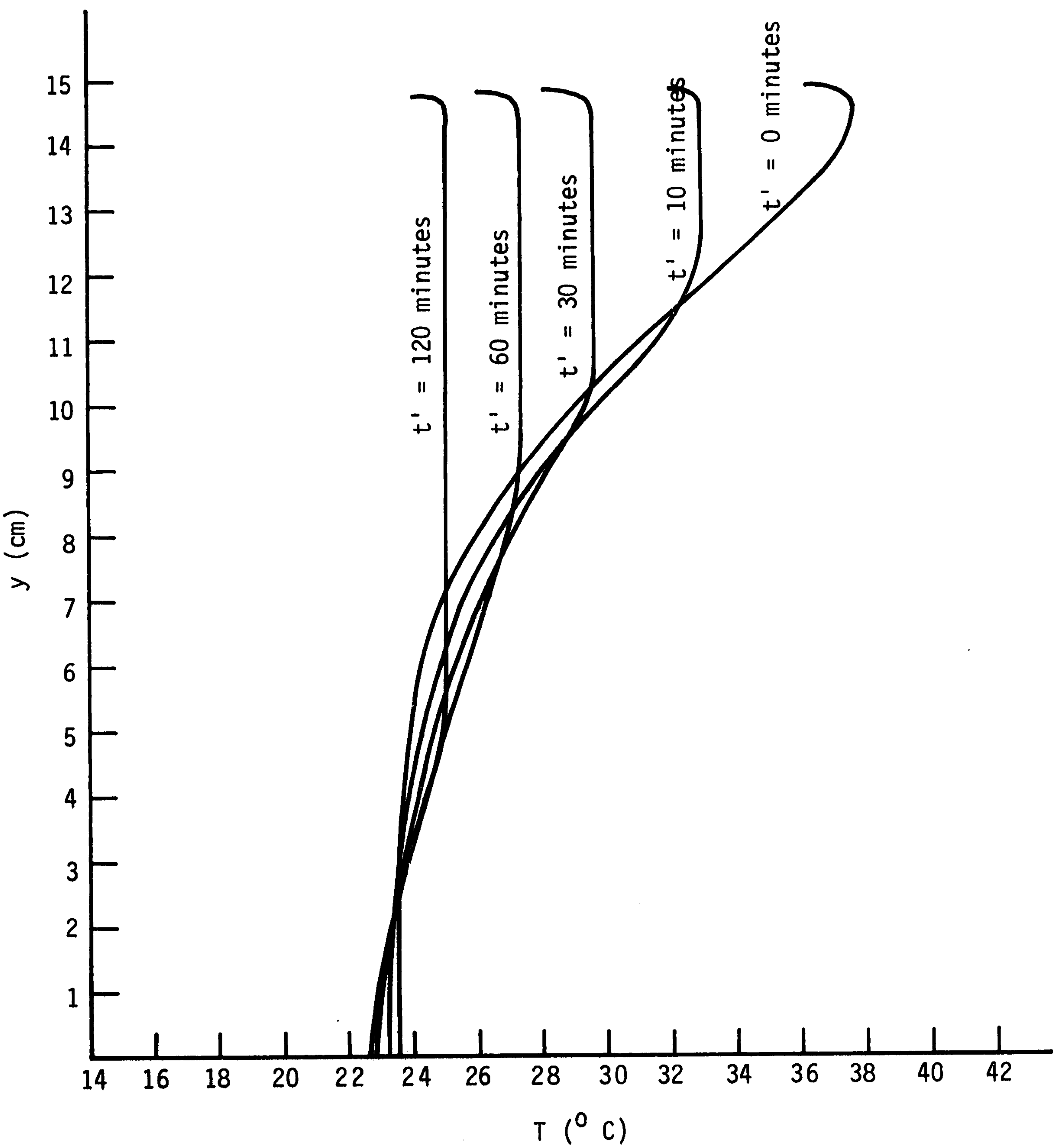

Fig. 18. Temperature Profiles for Run 10

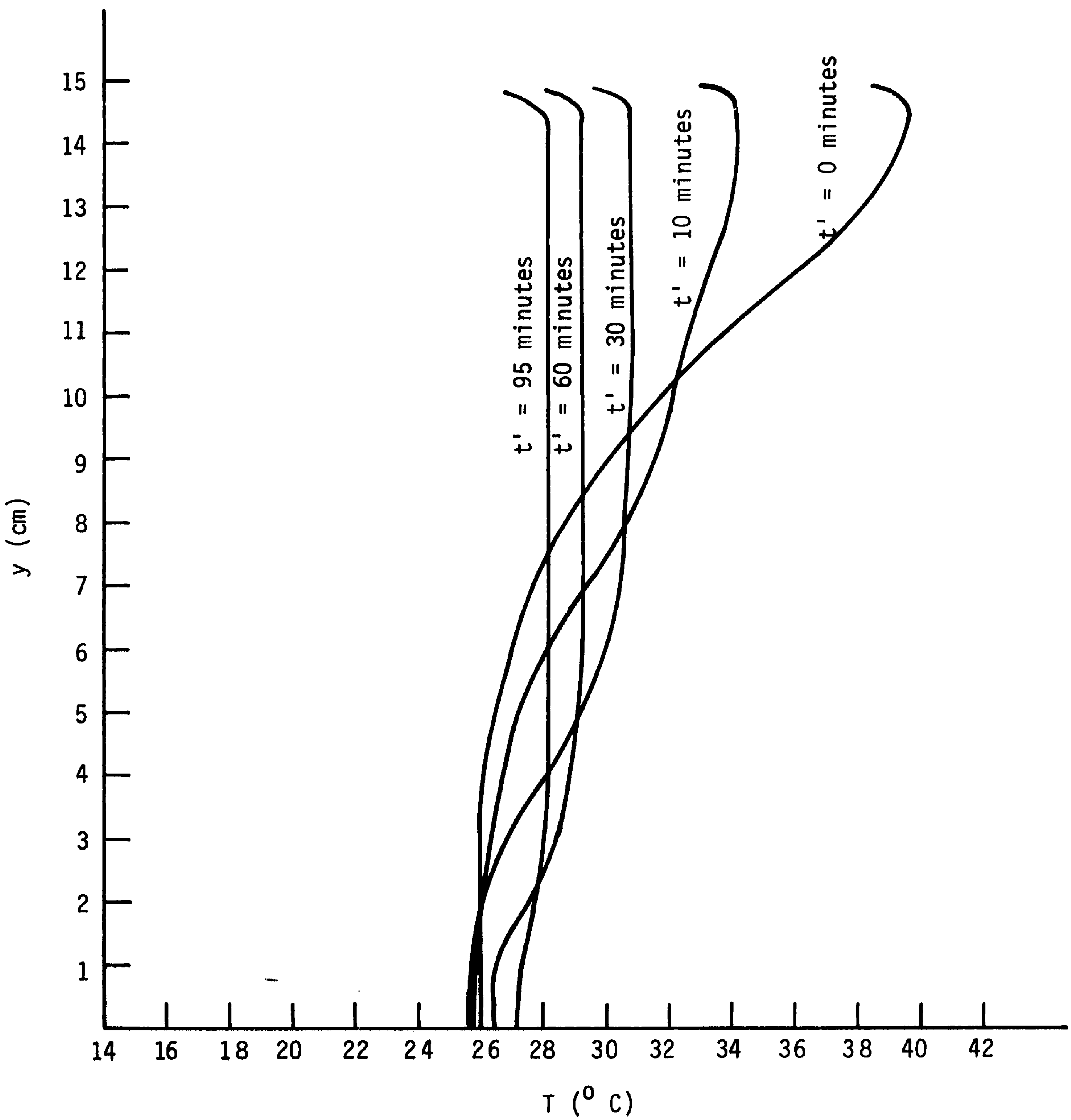

Fig. 19. Temperature Profiles for Run 11

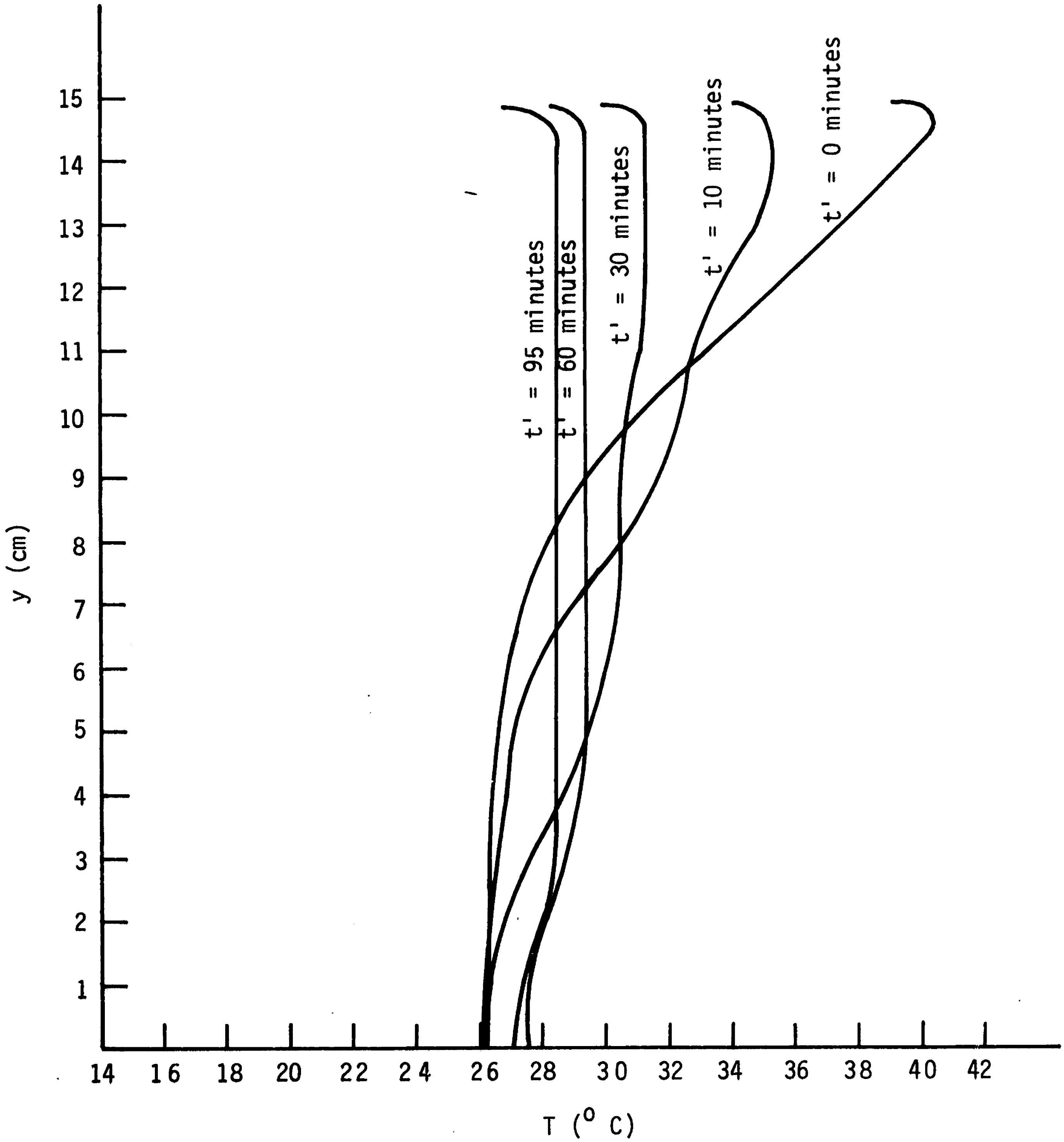

Fig. 20. Temperature Profiles for Run 12

B. Definitions and Data Reduction

1. Stability: The data obtained in this series of experiments was analyzed from an energy point of view. A measure of the state of stratification at any time was taken to be the stability, defined as the difference between the potential energy of the stratified body of water at a particular time and the potential energy which would exist in a body of water of equivalent mass, heat content, and free surface area with a uniform temperature distribution:

$$S = \int_A \left[\int_0^H \gamma(y) y \, dy \right] dA - \gamma_i A \frac{H_i^2}{2} \quad (1)$$

where:

S = Stability

$\gamma(y)$ = Specific weight of water at elevation y above false bottom

H = Depth of stratified body of water

A = Free surface area

γ_i = Specific weight of water if the temperature distribution were uniform and if the heat content and mass were the same as in the stratified case

H_i = Depth of water for case of uniform temperature distribution

γ_i and H_i may be determined as follows:

$$Q_H = \int_A \left[\int_0^H h(y) \, dy \right] dA \quad (2)$$

where:

Q_H = Heat content of body of water

$h(y)$ = Enthalpy per unit volume at elevation y

The enthalpy (defined as the internal energy excess over that of the fluid at some base temperature plus the work done on the system in changing the volume from that at the base temperature to that at the temperature in question) is used, rather than the specific heat times the temperature, because some change in volume would occur if the system were transformed from a stratified to an isothermal state without heat exchange. The equivalent isothermal enthalpy is

$$h_i = \frac{Q_H}{m_a} \tag{3}$$

where:

m_a = Mass of body of water $= \int_A \left[\int_0^H \rho(y)\, dy \right] dA$ where $\rho(y)$ is the fluid mass density at elevation y.

T_i, the equivalent uniform temperature may be obtained from tables of enthalpy vs. temperature. γ_i may be obtained from tables of specific weight vs. temperature, and H_i may be calculated by the following:

$$H_i = \frac{\gamma_i}{m_a g} A \tag{4}$$

where:

g = Gravitational acceleration

For purposes of calculation, all of the above integrals are converted into summations involving finite increments of y. This procedure is discussed in detail in Appendix A, Sample Calculations, and Appendix B, Sources of Error.

2. Stability which would have occurred without mixing: The change in stability which occurs during the mixing process is not, in itself, a correct measure of the effect of the induced mixing because some change in stability would have occurred during the same period of time without mixing. The change in the quantity S-S', where S' is the stability which would have existed without mixing, is a more reasonable measure of this effect.

Runs 1, 5, 6, and 10 were performed in order to determine S' as a function of time for different depths and radiation. A plot of stability vs. time for Run 1 and the first portion of Run 5 is shown in Fig. 21. The average of these two curves, shown in Fig. 22, was assumed to be representative of the stability behavior of the body of water with the lamps on and with a depth of 22 cm. For runs in which the lamps were left on during the gas injection phase, S' was determined for a particular time, t' minutes after the beginning of injection, by first locating S_0, the stability at t' = 0, on Fig. 22. S' for any time t' was taken to be the stability at time $t^o + t'$ (where t^o is defined as the time corresponding to S_0 on the graph). Figure 23 shows a schematic diagram of this technique:

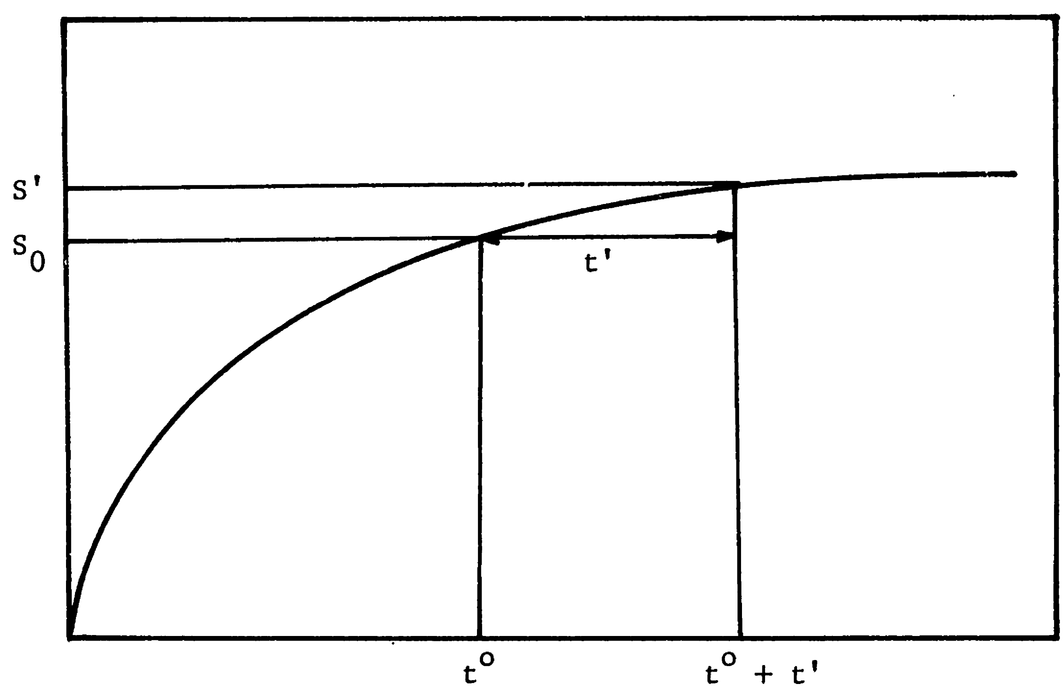

Fig. 23

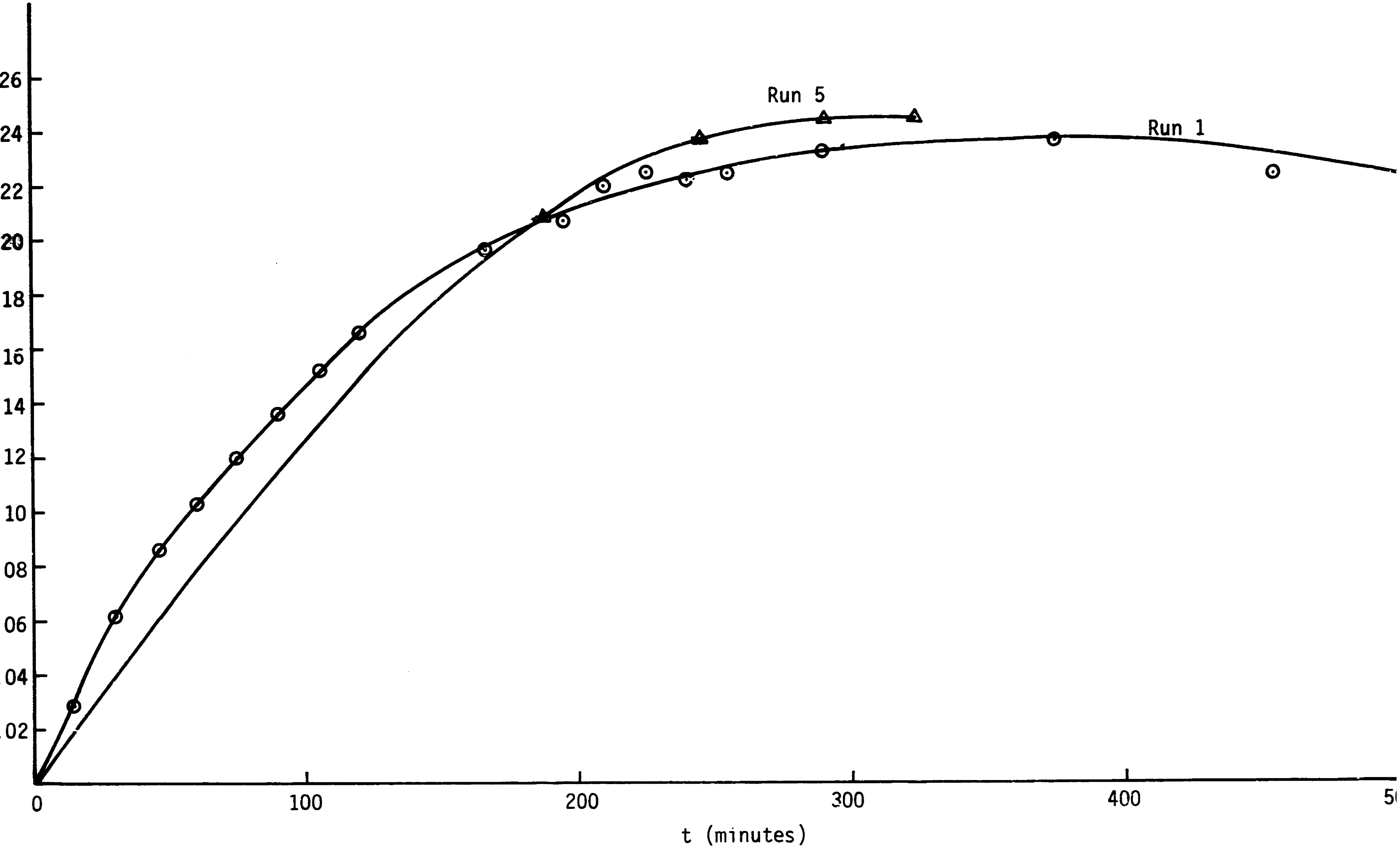

Fig. 21. Stability vs. Time for Runs 1 and 5

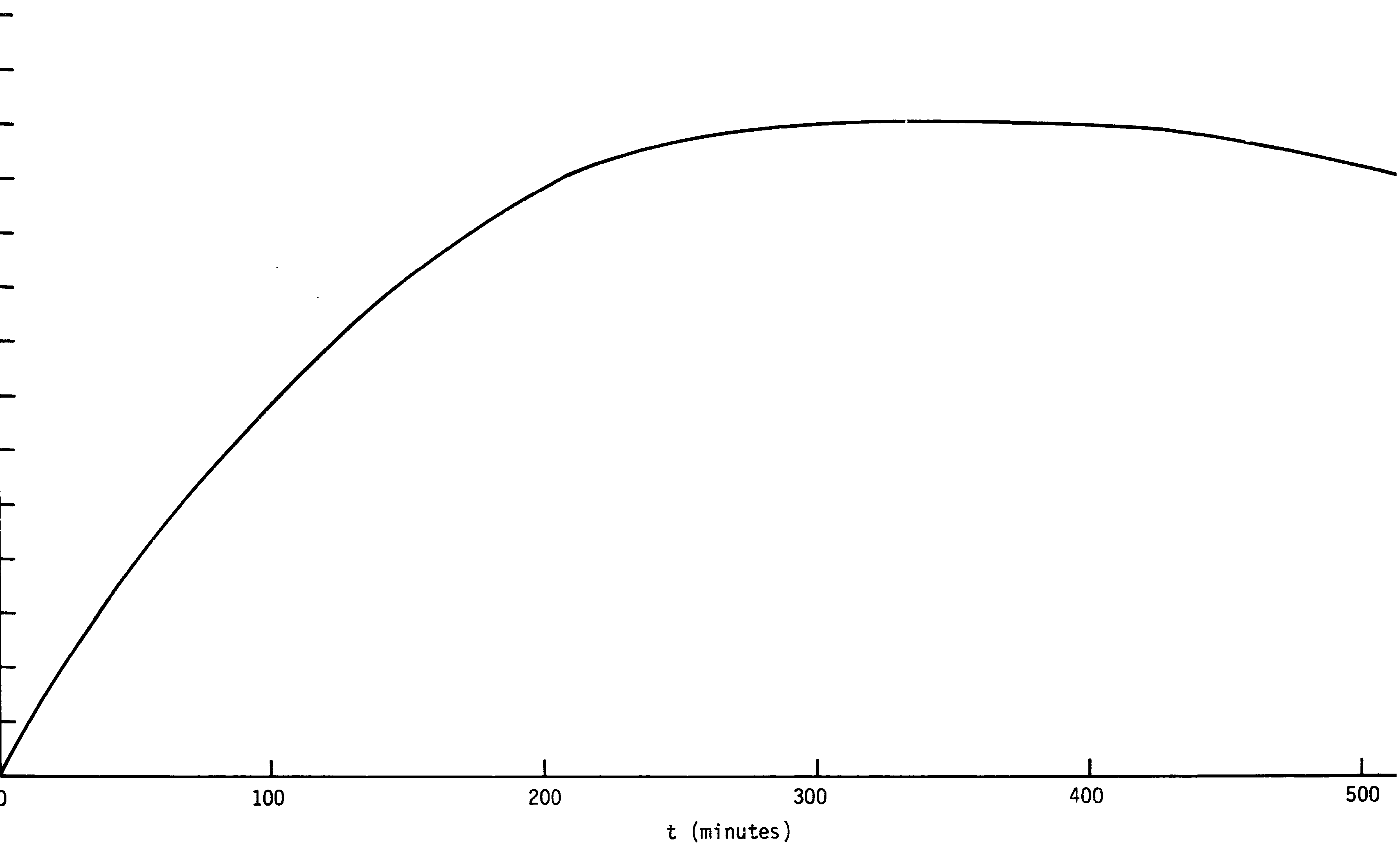

Fig. 22. Stability vs. Time with Lamps On

Runs 6 and 10 and the second portion of Run 5 were performed to determine the change in stability which results when the lamps are turned off and there is no gas injection. Figure 24 shows a plot of $(S/S_0)'$ vs. t' for these runs. t' is the time in minutes after the lamps were turned off; $(S/S_0)'$ is the stability at time t' divided by the stability at time t' = 0. Runs 5 and 6 were both at a depth of 22 cm, but their stabilities at the time the lamps were turned off were quite different. Since the curves for both runs are almost identical, it was assumed that for any initial stability, S_0, considered in these experiments, the curve $(S/S_0)'$ vs. t' would be the same. Figure 25 is a plot of the average of the curves for Runs 5 and 6.

To obtain S' at time t' for a particular run with initial stability S_0, depth of 22 cm, and with the lamps off during gas injection, the value of $(S/S_0)'$ for time t' on Fig. 25 was multiplied by S_0.

Run 10 was at a depth of 15 cm. Since the results of this run, plotted in Fig. 24, are significantly different from those of the other two runs, S' for this depth was determined using this curve rather than Fig. 25.

3. Per cent mixed: A measure of the relative amount of mixing achieved at any time t' after the beginning of gas injection was taken to be the per cent mixed, M, defined by

$$M = \frac{S - S'}{S'} \times 100 \qquad (5)$$

where M, S, and S' are functions of t'. Table 2 presents a listing of values of S, S', and M vs. time for each profile measured in Runs 1 through 12.

4. Efficiency: The efficiency of a system is defined as the ratio of a measure of the favorable output divided by a measure of the input.

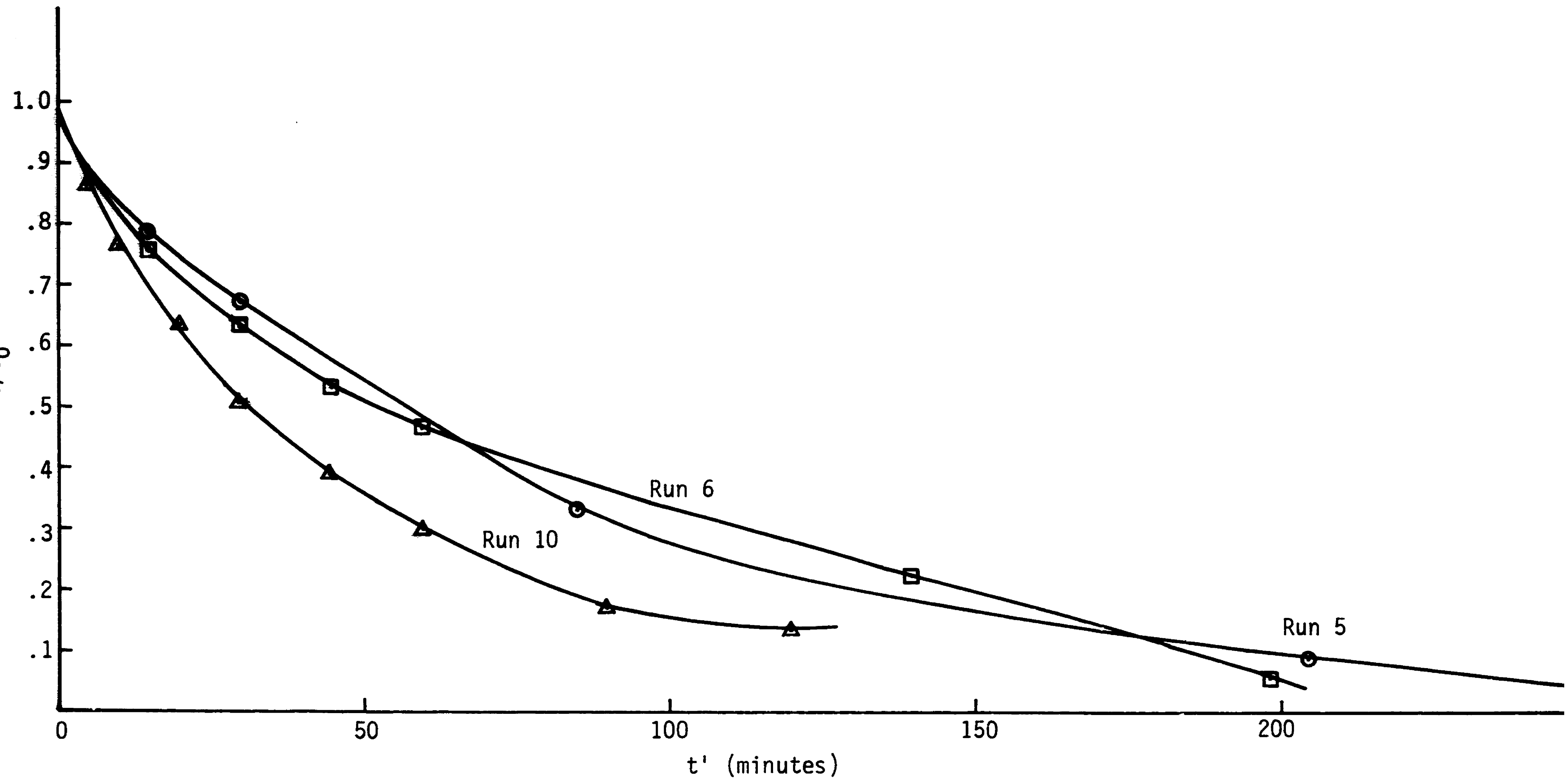

Fig. 24. Relative Stability vs. Time for Runs 5, 6, and 10

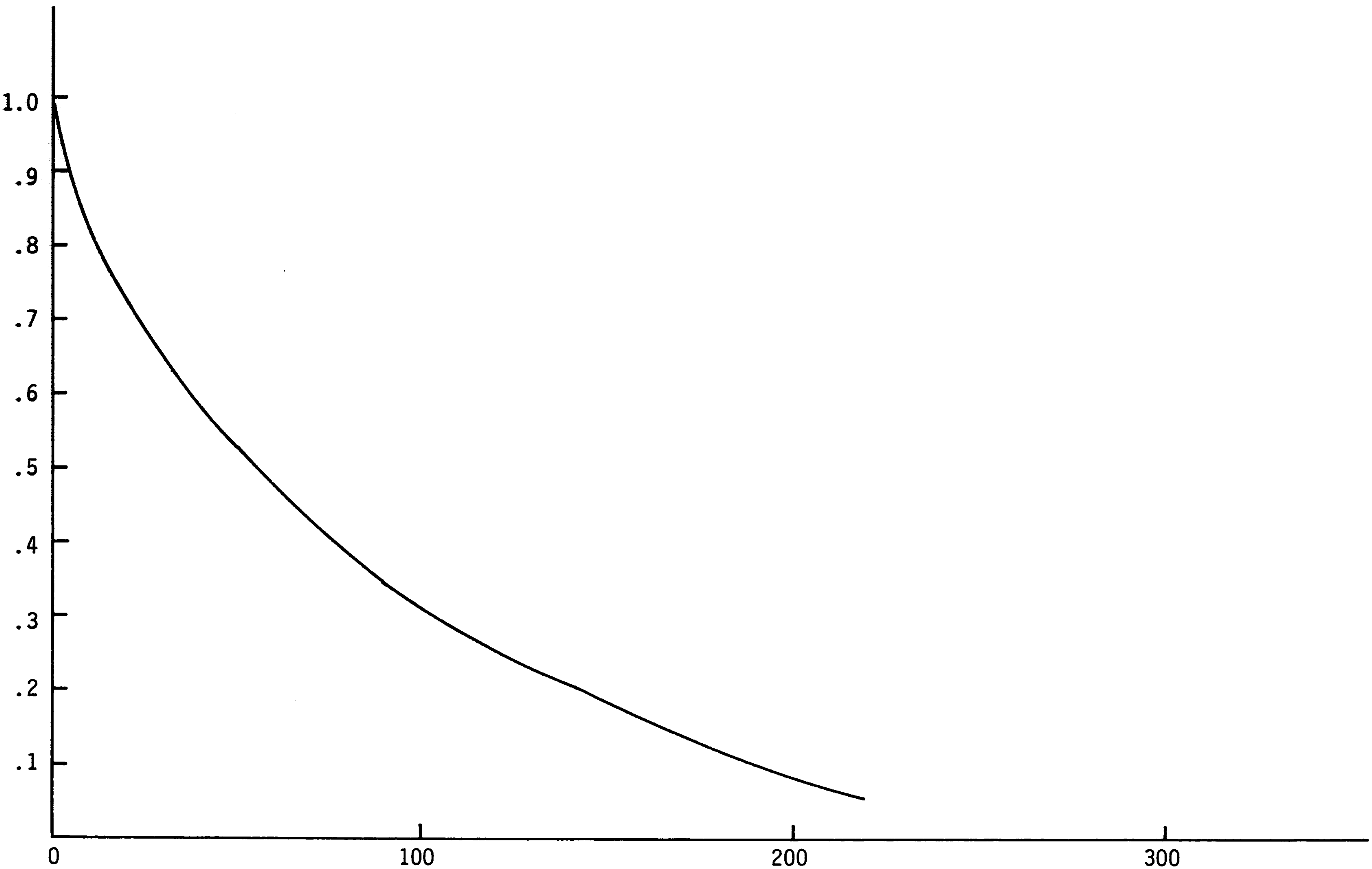

Fig. 25. Relative Stability vs. Time with Lights Off

TABLE 2

RUN	t (minutes)	t' (minutes)	S/gA (grams/cm)	S'/gA (grams/cm)	M (per cent)
1	0		0		
	15		.02811		
	30		.06175		
	45		.08534		
	60		.10291		
	75		.11955		
	90		.13551		
	105		.15155		
	120		.16305		
	167		.19579		
	195		.20756		
	210		.21981		
	225		.22406		
	240		.22038		
	255		.22413		
	290		.23295		
	375		.23725		
	455		.22460		
	510		.22889		
2	240	0	.22533	.225	0
		5	.19789	.208	1.6
		10	.13765	.191	25.5
		15	.12335	.179	28.8
		25	.08985	.159	43.0
		35	.07297	.143	47.2
		45	.05657	.129	54.2
		60	.04235	.112	60.5
		75	.03810	.091	57.8
		122	.00874	.056	84.5
		178	.00241	.027	91.8
3	235	0	.21964	.219	0
		5	.18557	.196	5.3
		10	.14080	.180	21.4
		20	.11395	.159	29.8
		30	.08755	.143	38.4
		45	.06593	.122	46.8
		60	.04777	.105	54.2
		90	.02945	.075	60.2
		120	.01316	.055	76.0

TABLE 2 (cont.)

RUN	t	t'	S/gA	S'/gA	M
4	207	0	.20550	.205	0
		5	.18176	.184	1.3
		10	.12907	.169	28.2
		20	.10343	.150	30.8
		30	.06159	.134	53.9
		45	.04525	.114	60.1
		60	.02697	.098	72.8
		90	.01056	.070	84.9
		120	.00564	.052	89.0
5	0		.00000		
	188		.20915		
	245		.23762		
	291		.24244		
	323	0	.24228		
	338	15	.19139		
	353	30	.16313		
	408	85	.08023		
	528	205	.02275		
	568	245	.01159		
6	171	0	.20557		
		17	.15432		
		30	.13095		
		45	.10917		
		60	.09682		
		141	.04602		
		199	.01298		
7	0	0	.00000	.000	0
	5	5	.00324	.010	
	15	15	.02758	.030	6.7
	30	30	.04428	.062	29.0
	45	45	.05863	.085	30.6
	60	60	.06435	.102	37.2
	90	90	.08295	.135	39.2
	120	120	.07917	.166	52.5
	162	162	.06932	.196	64.9
	248	248	.06196	.225	72.5

TABLE 2 (cont.)

RUN	t	t'	S/gA	S'/gA	M
8	195	0	.21380	.213	0
		5	.17753	.213	17.4
		10	.16589	.214	24.7
		20	.15920	.217	27.4
		30	.13912	.220	37.5
		45	.11701	.223	48.0
		60	.10674	.226	49.2
		75	.10510	.229	55.0
		90	.10387	.231	56.0
		182	.09884	.237	58.2
		270	.08452	.230	64.0
9	257	0	.21336	.213	0
		5	.18224	.190	3.6
		10	.14617	.174	15.8
		20	.10750	.154	30.5
		30	.08151	.138	42.3
		45	.05630	.118	52.2
		60	.04551	.101	56.2
		75	.03767	.085	56.1
		90	.01686	.072	73.7
10	0		.00000		
	15		.02518		
	60		.06280		
	90		.07468		
	120		.08649		
	150		.09346		
	165		.09426		
	180		.09579		
	191	5	.08299		
	196	10	.07375		
	206	20	.06090		
	216	30	.04849		
	231	45	.03761		
	246	60	.02875		
	276	90	.01659		
	306	120	.01371		

TABLE 2 (cont.)

RUN	t	t'	S/gA	S'/gA	M
11	190	0	.09601	.096	0
		5	.07584	.083	8.8
		10	.06097	.074	17.6
		20	.04439	.061	27.2
		30	.03138	.049	35.4
		45	.01936	.038	48.6
		60	.01220	.029	57.1
		95	.00361	.015	76.1
12	175	0	.08854	.088	0
		5	.07941	.076	3.7
		10	.06770	.068	
		20	.04638	.056	17.8
		30	.03133	.044	30.1
		45	.01853	.035	46.6
		60	.00976	.026	63.2
		95	.00360	.014	74.5

For the system considered here, a good measure of the output at any time is the quantity S - S'. A measure of the input is the energy delivered to the system by the nitrogen entering through the nozzle.

$$E_i = \rho_n Q t' \frac{V^2}{2} + pQt' \tag{6}$$

where:

- E_i = Energy input
- ρ_n = Gas density
- Q = Gas volume flow rate
- t' = Time after beginning of injection
- V = Velocity of gas at nozzle = $\frac{Q}{a}$, where a is the area of the nozzle
- p = Hydrostatic pressure at nozzle = $\gamma_i(H-z_o)$, where z_o = height of nozzle above false bottom, and γ_i = average specific weight of water

Q is determined from the flow meter reading according to the equation

$$Q = \frac{\mu_o}{\mu} Q_1 \tag{7}$$

where:

- Q_1 = Meter reading
- μ_o = Dynamic gas viscosity at standard temperature and pressure
- μ = Dynamic gas viscosity at the flow meter temperature and internal pressure

The efficiency, η, is defined as follows:

$$\eta = \frac{S - S'}{E_i} \tag{8}$$

All of these quantities are functions of t'. In order to compare the efficiencies of different systems, it is necessary to select a particular value of t' at which this comparison is to be made. For these experiments, the time selected was t'_{50}, defined as the value of t' corresponding to M = 50%. A plot of η at t'_{50}, defined as η_{50}, vs. Q is presented in Fig. 26. The data points shown include all of Brainard's and all of those for the present investigation for which the depth was 22 cm. The upper set of points corresponds to the case in which the lamps were left on during injection, and the lower set corresponds to leaving the lamps off.

C. Effect of Radiation During Gas Injection

As was seen in Fig. 26, the value of η_{50} calculated for a particular system varies considerably depending upon whether or not the lamps were left on during the mixing phase. This is further illustrated by Fig. 27, in which η is plotted vs. t' for two runs which differed only with regard to the radiation being received during the gas injection phase. The experiment in which the lamps were left on yielded consistently higher values of η than did the experiment with lamps off.

Figure 28 shows a plot of M vs. t' for the same two runs. As may be seen, the two curves are practically identical for the first 100 minutes of mixing. The effect of the amount of radiation being received during injection is not apparent for this period of time.

D. Quantities Required for Design

In the design situation, the quantities which the engineer would need to predict are the time and power required in order to achieve a certain amount of mixing with a particular system. If a gas injection scheme is chosen for destratification of a particular reservoir at a particular time, then essentially the only quantity which may be varied is the gas flow rate. As was seen in Fig. 26, the efficiency does not

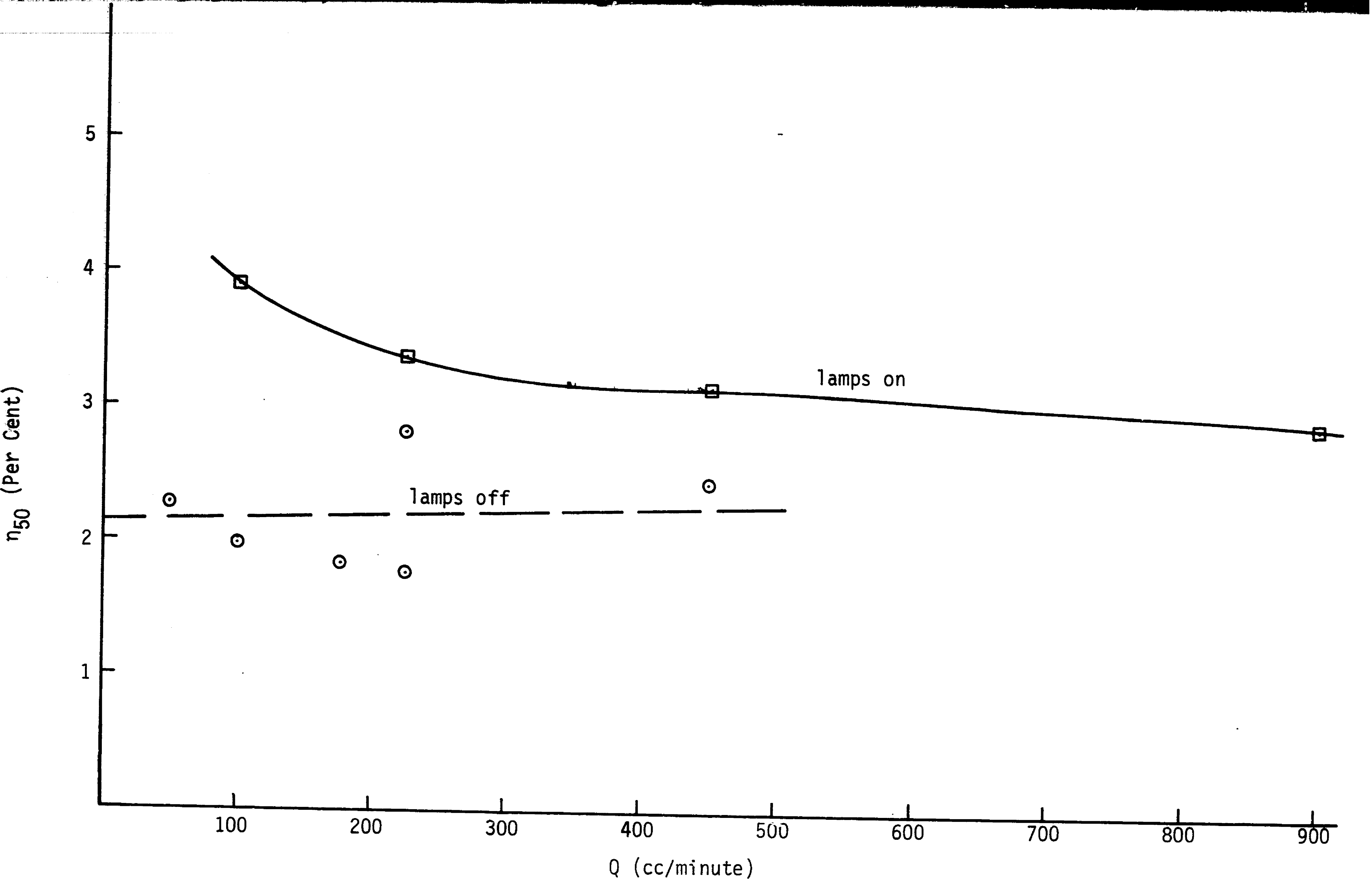

Fig. 26. η_{50} vs. Q for All Runs with H = 22 cm

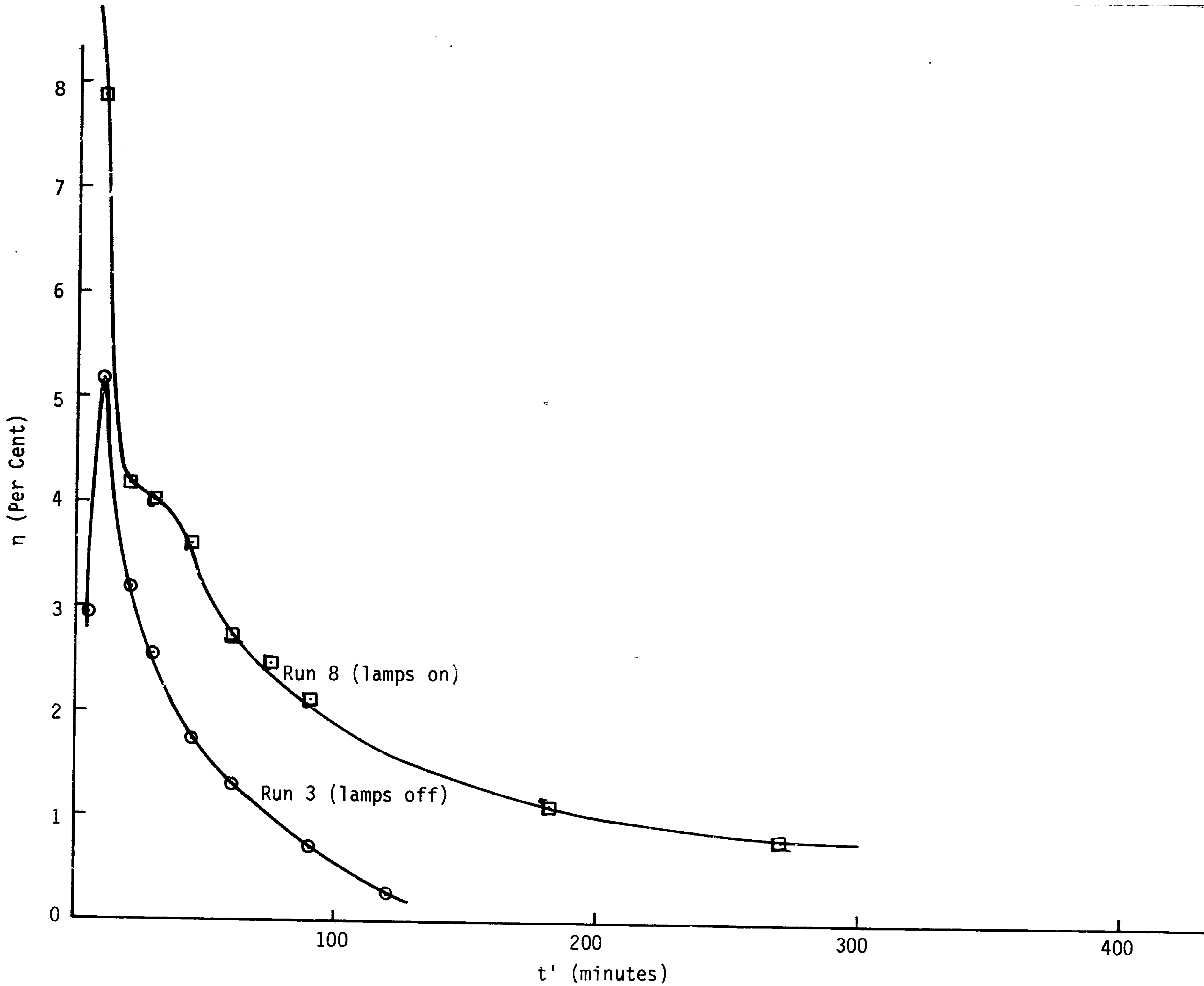

Fig. 27. η vs. t' for Runs 3 and 8

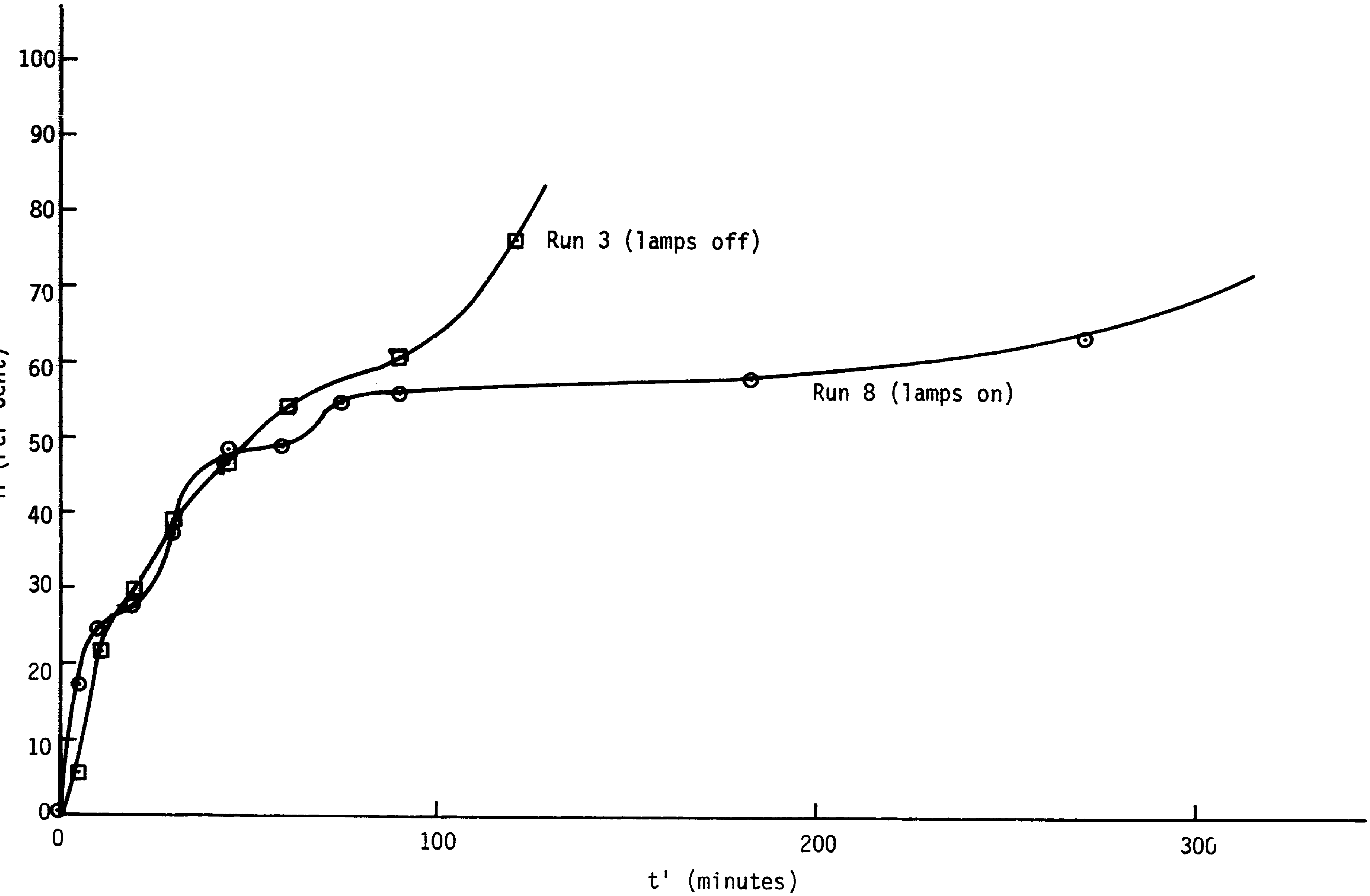

Fig. 28. Per Cent Mixed vs. Time for Runs 3 and 8

vary greatly with flow rate. Therefore, the power consumed by the system will be essentially constant for all values of Q. The most important design quantity, therefore, is the amount of time required for each mixing scheme. For this reason, and because η varies depending upon the radiation being received during the mixing phase, the remainder of this report will be concerned with the times involved in attaining certain degrees of destratification rather than the efficiencies of the processes.

E. Logarithmic M-t' Curves

A convenient form for presenting the data for these experiments is to plot M vs. log t'. These curves are approximately linear for most values of M and they may be expressed analytically by

$$M = B \log \frac{t'}{t'_o} \quad (9)$$

where:

B = Slope of linear portion of curve

t'_o = Intercept of extension of linear section with horizontal axis

Curves of M vs. log t' for all of the gas injection runs of this series of experiments and also for all of Brainard's runs (5B, 7B, 8B, 9B, and 10B) are shown in Figs. 29 through 34.

A summary of values of Q, B, t'_o, t'_{50}, H, and Qxt'_{50} for these experiments is presented in Table 3.

F. Field Results

A reasonably large amount of data is available for various field testing programs involving induced mixing in thermally stratified lakes and reservoirs. For this analysis, five sets of field data will be considered. Field tests 1 through 3 are reported in Ref. 11; and Field

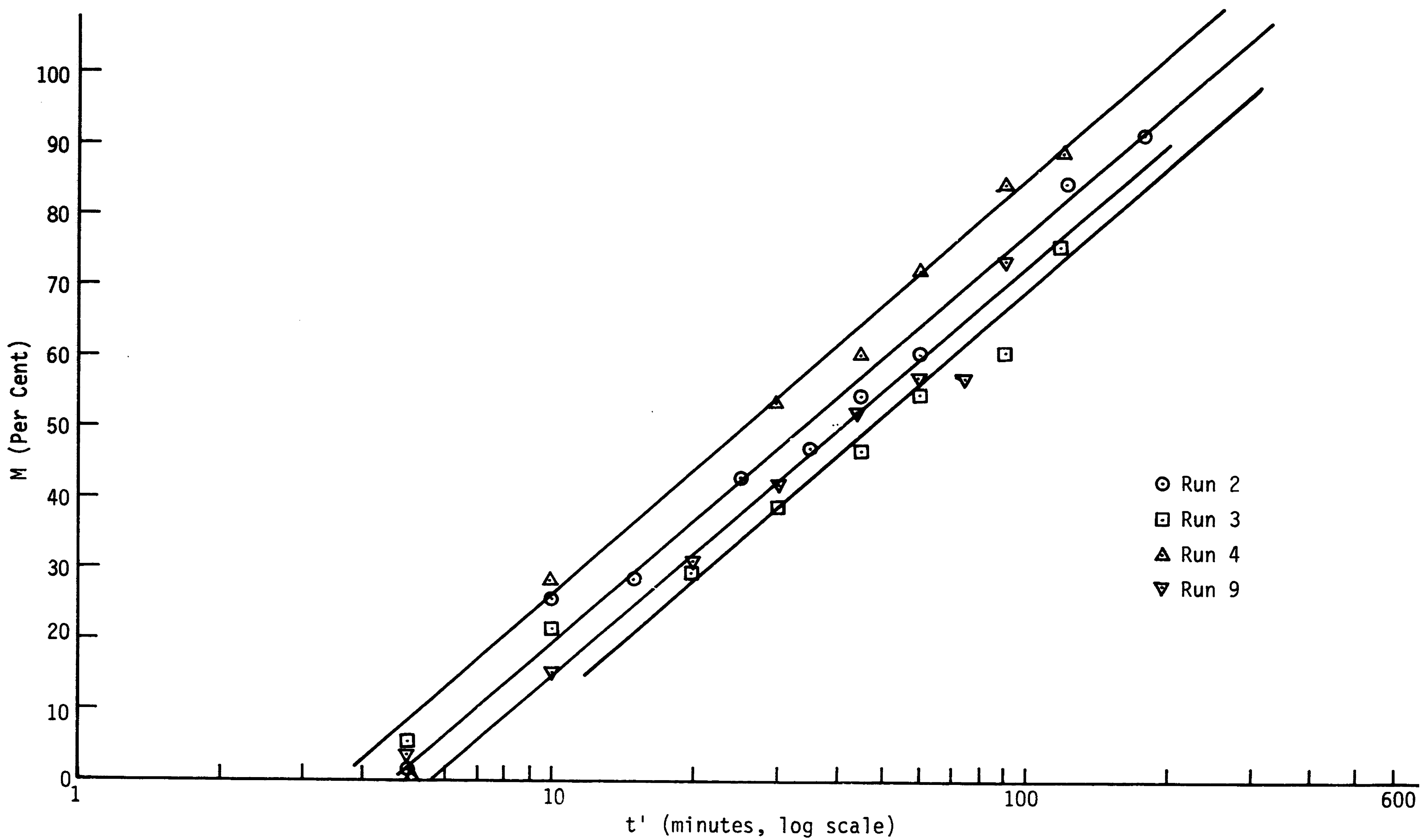

Fig. 29. Per Cent Mixed vs. Time for Runs 2, 3, 4, and 9

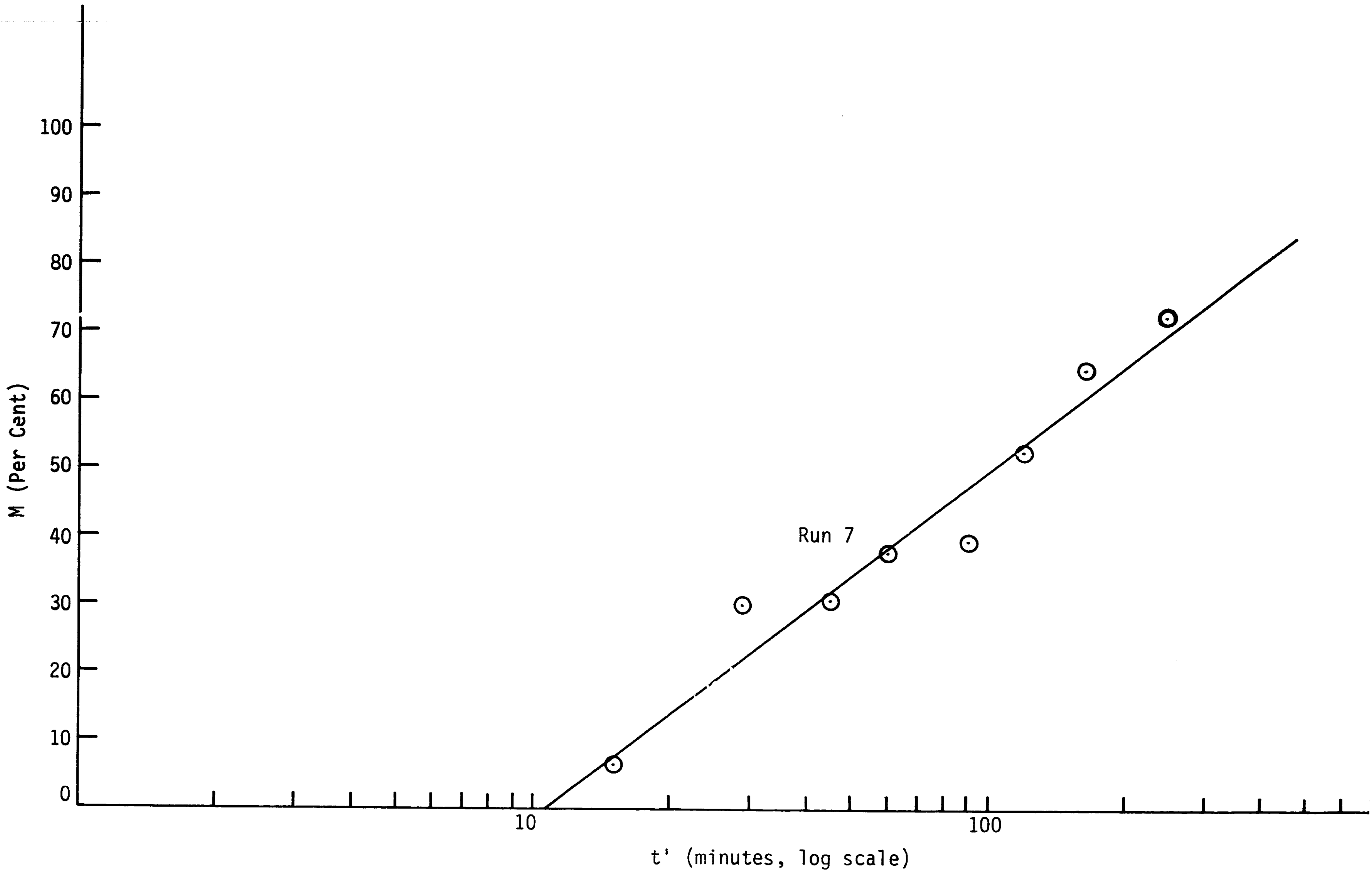

Fig. 30. Per Cent Mixed vs. Time for Run 7

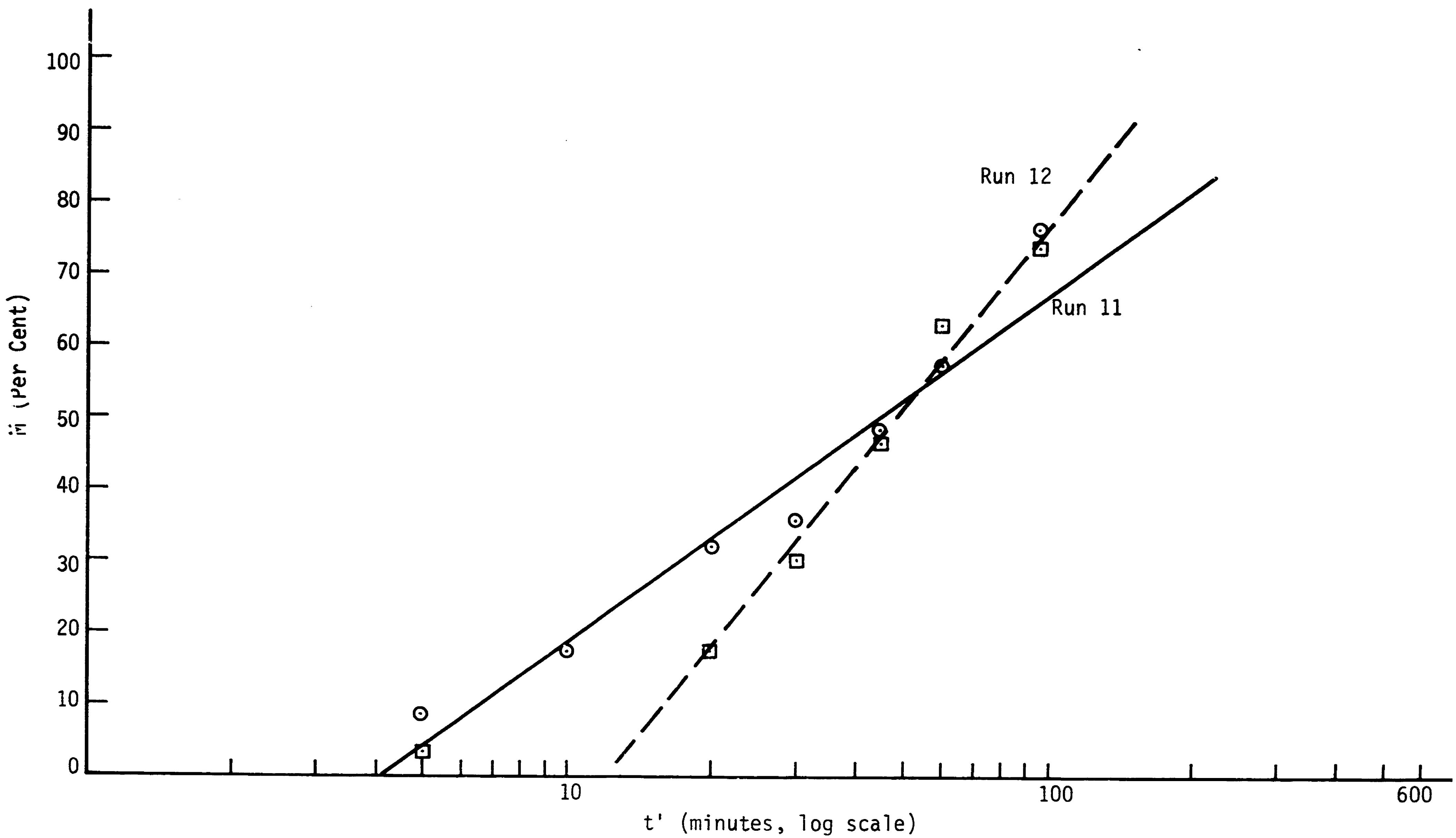

Fig. 31. Per Cent Mixed vs. Time for Runs 11 and 12

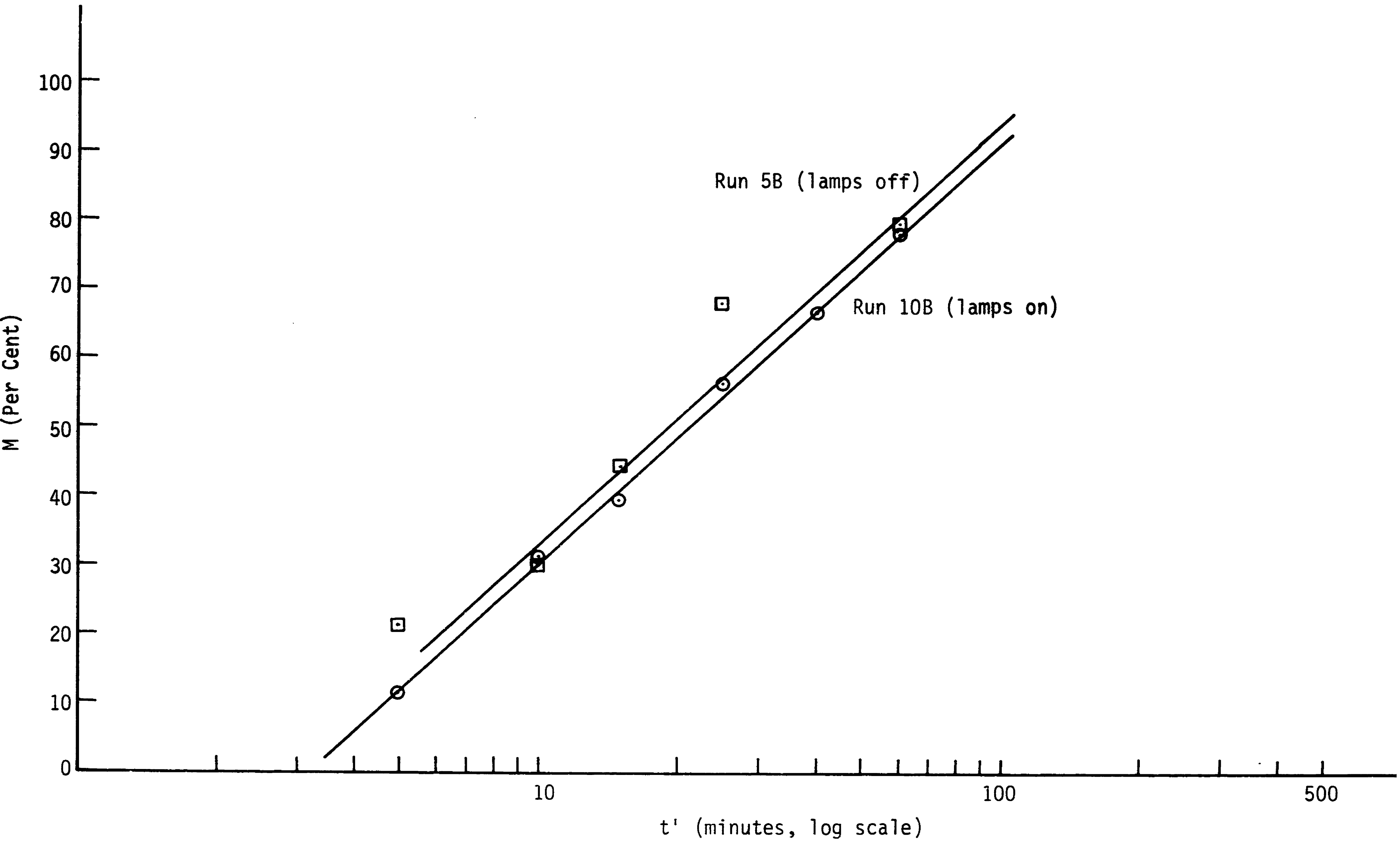

Fig. 32. Per Cent Mixed vs. Time for Runs 5B and 10B

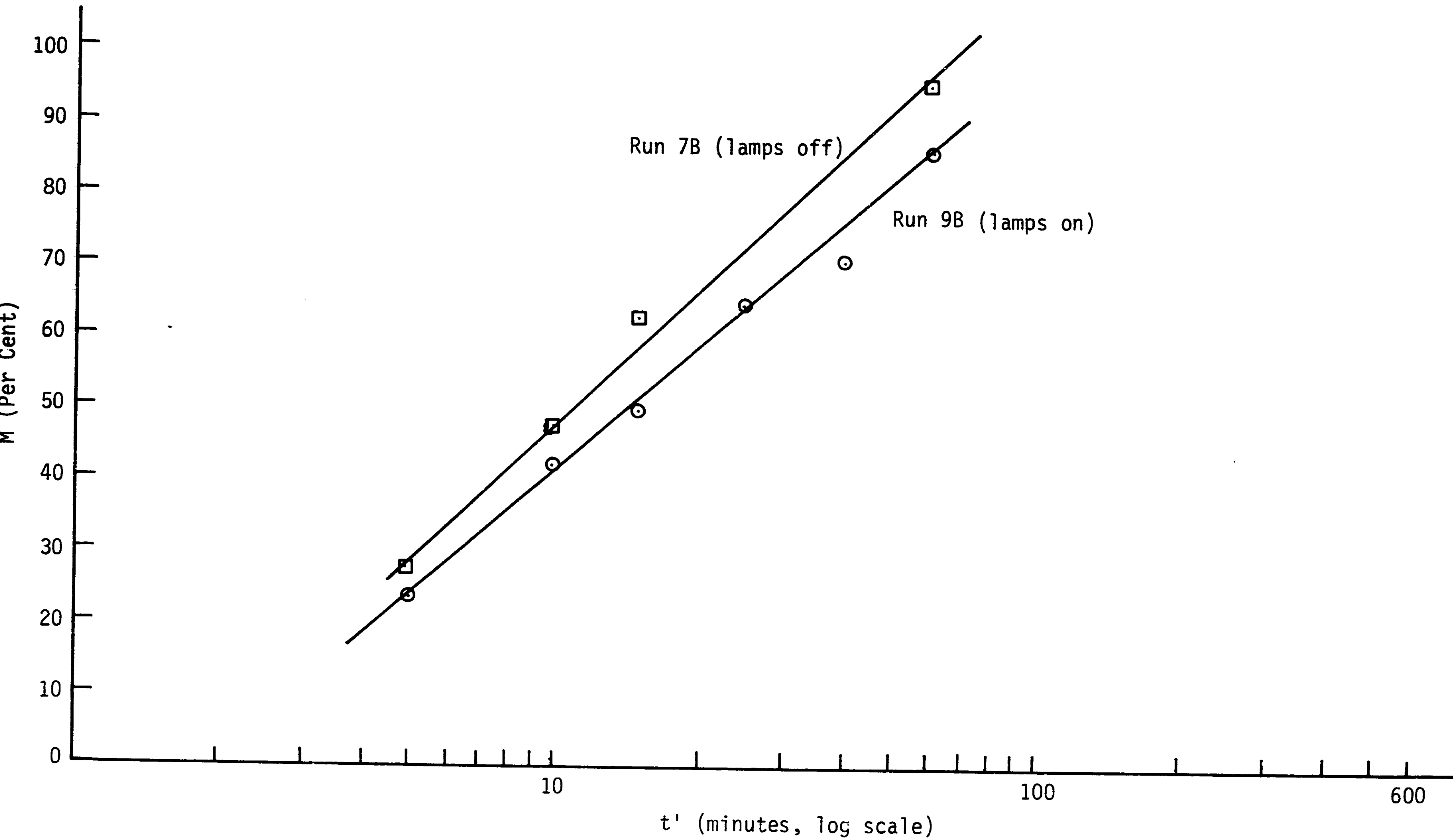

Fig. 33. Per Cent Mixed vs. Time for Runs 7B and 9B

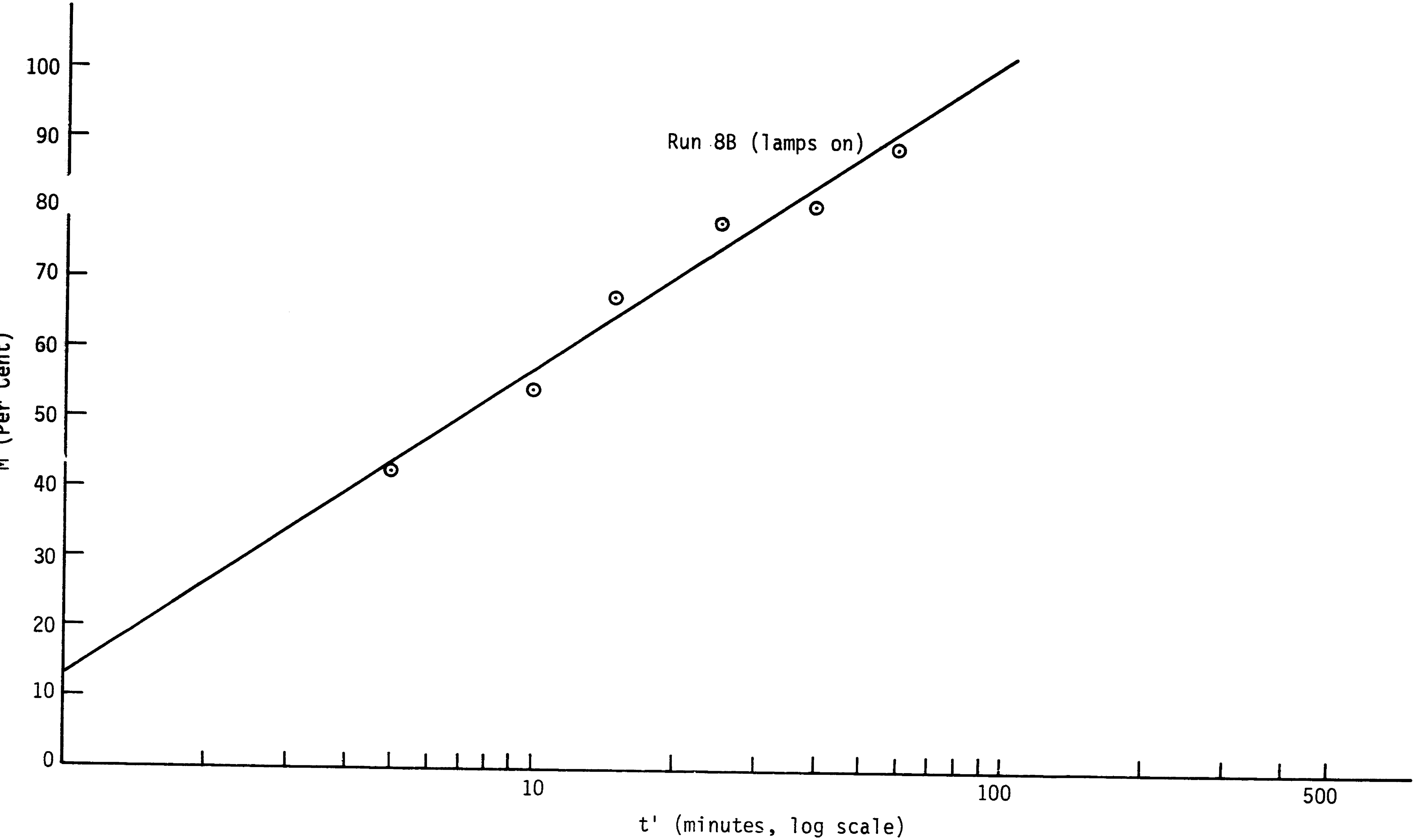

Fig. 34. Per Cent Mixed vs. Time for Run 8B

RUN NUMBER	Q (cc/minute)	t'_o (minutes)	t'_{50} (minutes)	B	H (cm)	Qt'_{50} (cc)
2	175	4.6	34.0	58	22	5955
3,8	100	6.4	47.0	59	22	4700
4	250	3.5	25.5	59	22	6375
7	100	10.0	100.0	50	22	10,000
9	75	5.6	51.0	57	22	3825
11	250	4.1	58.0	49	15	14,500
12	100	12.0	56.0	90	15	5600
5B,10B	250	3.2	20.0	62	22	5000
7B,9B	450	1.9	12.5	59	22	5625
8B	900	0.5	6.9	44	22	6210

TABLE 3

tests 4 and 5 in Ref. 12. Field test 1 involved a scheme in which water was pumped from the bottom to the surface. Field tests 2, 3, 4, and 5 involved a scheme of gas injection similar to that employed in these laboratory tests. Field tests 1, 2, 3, and 4 were performed on well-stratified reservoirs which had not been mixed previously during the year. Field test 5 was performed on the same reservoir and during the same year as Field test 4. The stratification had only partly reformed after the first mixing.

The data for these field tests is presented in Figs. 35 through 38. In addition, the pertinent parameters for each test are listed in Table 4.

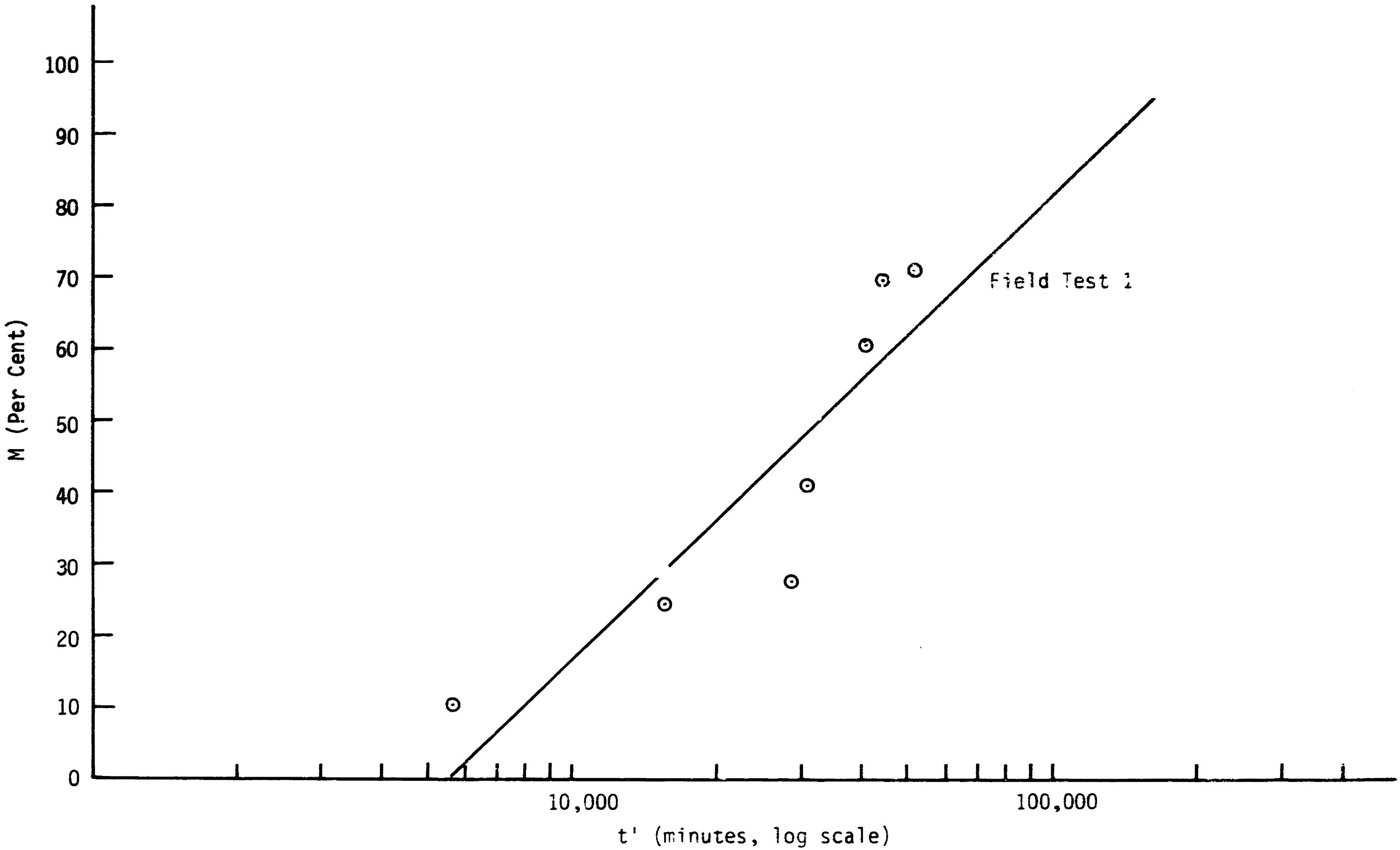

Fig. 35. Per Cent Mixed vs. t' for Field Test 1

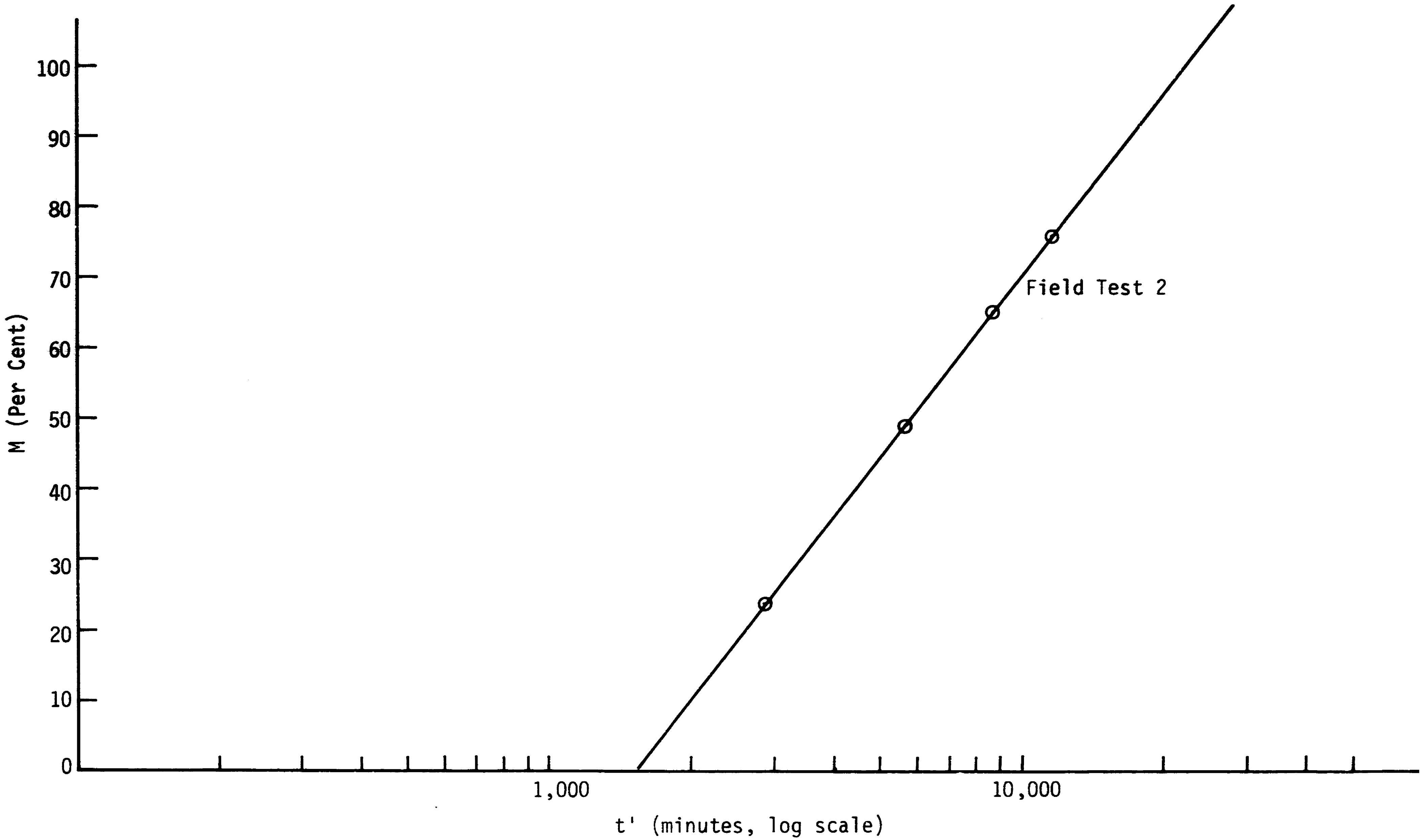

Fig. 36. Per Cent Mixed vs. t' for Field Test 2

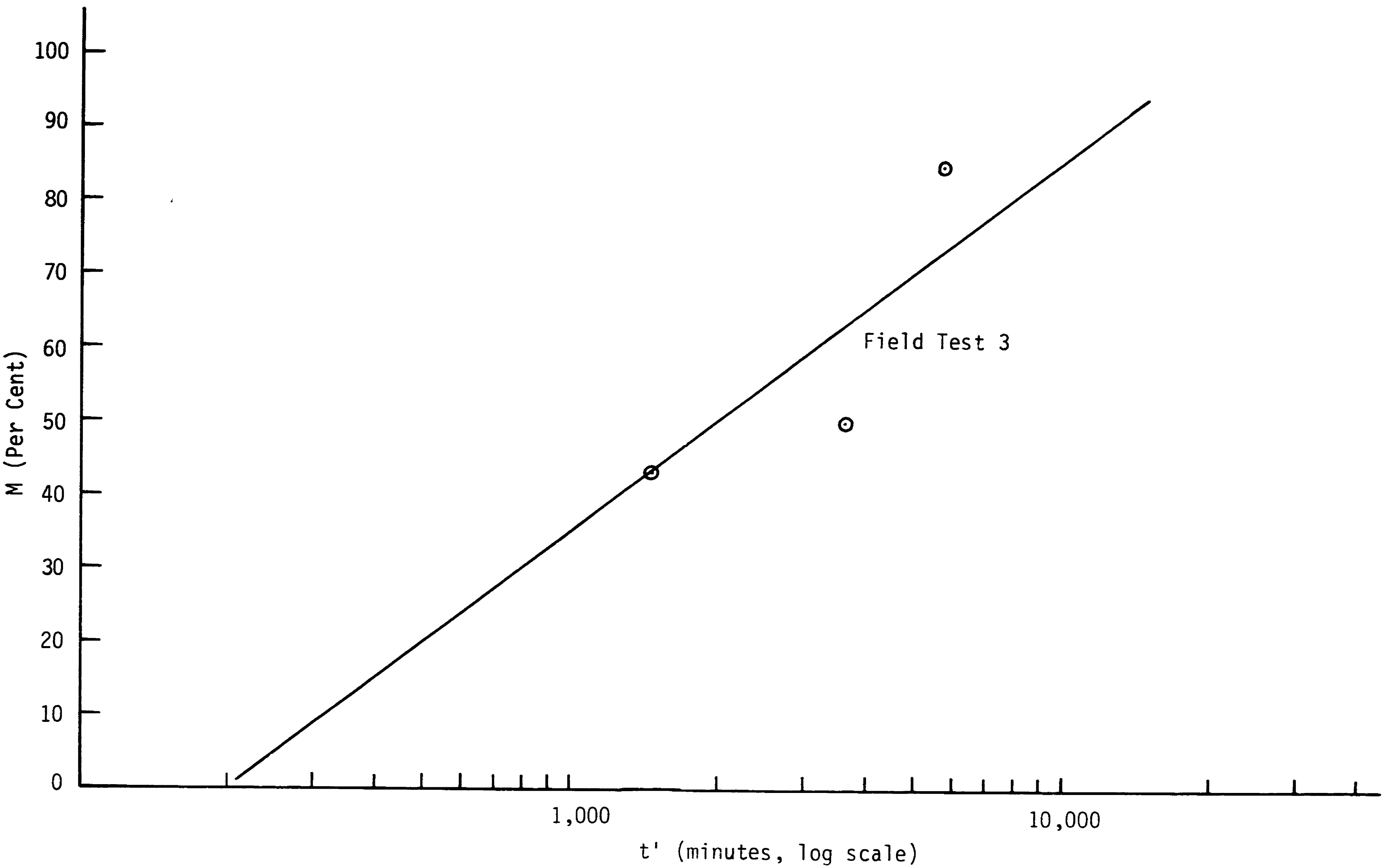

Fig. 37. Per Cent Mixed vs. t' for Field Test 3

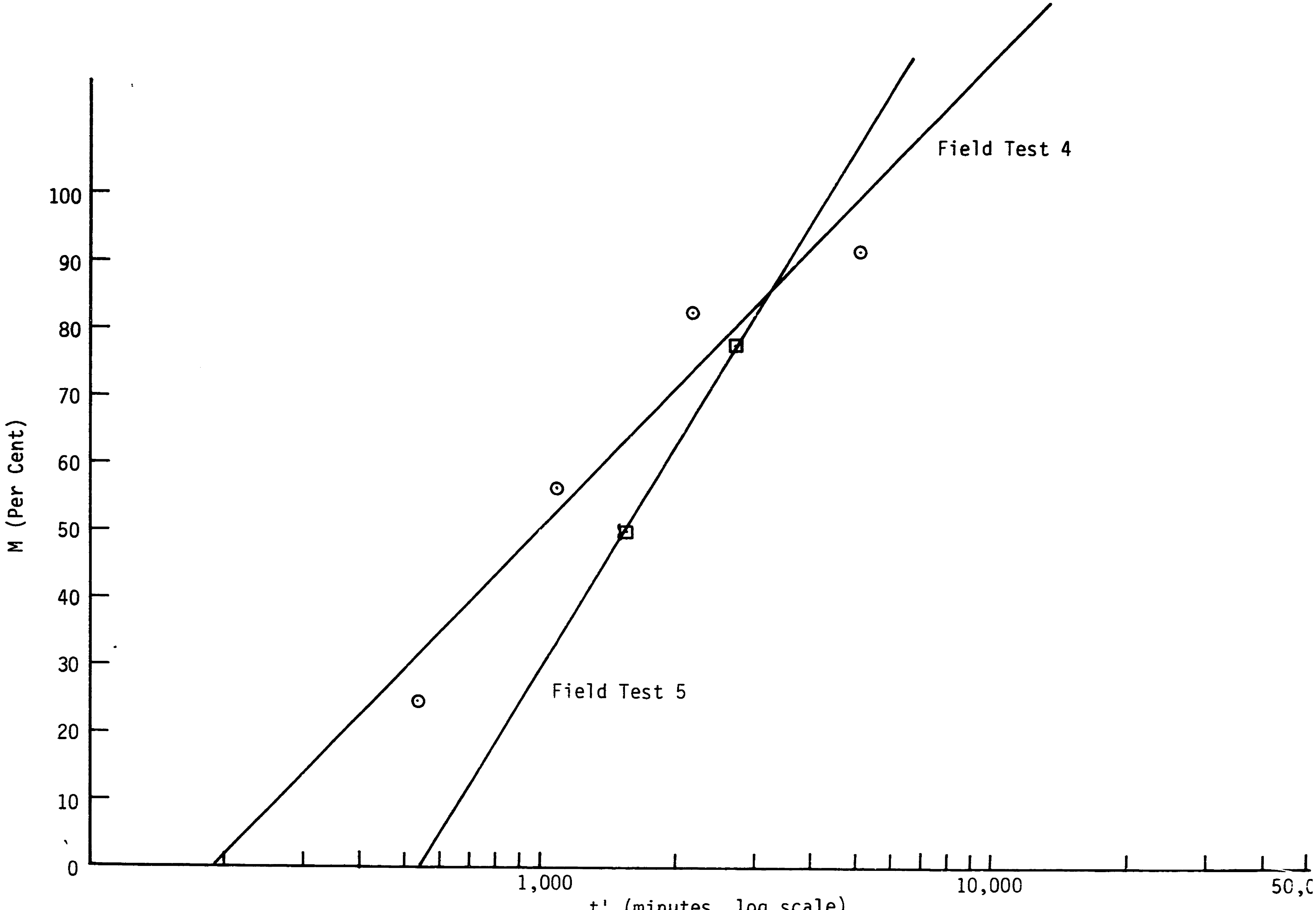

Fig. 38. Per Cent Mixed vs. t' for Field Tests 4 and 5

FIELD TEST #	DATE	RESERVOIR	Q (cc/min)	B	t'_o (min)	t'_{50} (min)	Qt'_{50} (cc)	AIR OR WATER PUMPING	A (cm^2)	H_{av} (cm)
1	8/65	Boltz Lake, Ky	1.12×10^7	55	5500	33,000	3.66×10^{11}	water	3.9×10^9	944
2	7/66	Falmouth Lake, Ky	3.27×10^6	85	1500	5800	1.90×10^{10}	air	9.1×10^9	608
3	6/66	Boltz Lake, Ky	3.18×10^6	51	190	2000	6.36×10^9	air	3.9×10^9	944
4	4/66	Lake Wohlford, Ca	5.96×10^6	70	190	1000	5.96×10^9	air	5.26×10^9	586
5	7/66	Lake Wohlford, Ca	5.96×10^6	90	520	1500	8.92×10^9	air	5.26×10^9	586

TABLE 4

VII. ANALYSIS OF RESULTS

A. Repeatability of Results

Run number 4 was performed in order to determine how closely Brainard's run number 5B could be reproduced. As may be seen in Table 3, the values of t'_o differ by about 5%. It may be concluded that results are reproducible within about this range.

B. Effect of Starting Mixing Early in the Spring

It has been suggested[11] that a reasonable scheme for eliminating thermal stratification in the summer would be to begin mixing in the spring and thereby prevent the stratification from ever developing. Run 7 was performed in order to check the efficiency of such an operation. The lamps and the gas injector were turned on at the same time and temperature profiles were measured. As Table 3 shows, a significantly larger t'_{50} resulted for this case. Also, by noting the temperature profiles in Fig. 15, it is evident that a certain amount of stratification must form before the mixing process can become effective. For the field situation, therefore, it would seem more reasonable to begin mixing late in the spring, after the development of a certain amount of stratification, but before any serious adverse side effects can develop.

C. Slope of M - log t' Curves

For all of the laboratory experimental results (except for Run 12), the value of B is practically constant and equal to about 55. For the field tests, B increases only slightly to a mean value of 70. For design purposes, either one of these values, or an average of the two, could be used. With B known, only one more parameter, such as t'_{50}, would need to be predicted in order to define the response of a reservoir to mixing induced by gas injection.

D. Effect of Q on t'_{50}

As would be expected, t'_{50} increases as Q decreases. It is also apparent from Table 3 that, at least for H = 22 cm, the product Q x t'_{50} is approximately constant. There is a slight tendency toward an increase in Q x t'_{50} for increasing values of Q, but this effect appears to be secondary. For H = 15 cm, only two experiments were run and no clear trends are apparent.

E. Effect of Initial Stability

The effect of varying the initial stability was not determined by a controlled set of experiments. However, a certain amount may be learned about this subject by examining the data presented here. In Fig. 24, the plots of S/S_0 vs. t' for Runs 5 and 6 are essentially identical, although the initial stability for Run 5 is about 1.2 times that of Run 6. Since these tests did not involve induced mixing, the only conclusion which may be reached is that the scheme for calculating S' as a function of t' which was developed earlier yields results which are not a function of initial stability.

Field tests 4 and 5 were run under approximately similar conditions, except the initial stability for Field test 4 was about 1.7 times that for Field test 5. The plots of M vs. log t' for these tests (Fig. 38) show that for large values of t' the values of M are similar, while for lower values of t' the curves diverge. Since the engineer would be primarily interested in large values of M, the difference between these two results is not great.

Runs 7 and 8 were run under similar conditions, except Run 7 had an initial stability of 0, while the initial stability per unit area for Run 8 was about 190 dynes/cm (well-formed stratification). Run 8 yielded a t'_{50} of about 50 minutes, while the t'_{50} for Run 7 was about 100 minutes. In this extreme case, the effect of the initial stability was rather strong.

In general it may be concluded that for cases in which the initial stratification pattern is not well-formed, the effect of the initial stability is often strong. For cases of well-formed stratification, the effect of initial stability seems to be considerably less.

F. Prediction of Field Results on the Basis of Laboratory Tests

Probably the most important quantity which the engineer would need to estimate for the design of an induced mixing system is t'_{50}. This parameter is probably a function of numerous quantities, including flow rate, type of mixing scheme (water or gas), reservoir size (average depth, surface area), reservoir shape (circular, elliptical, etc.), initial temperature profile, air temperature, barometric pressure, and so on. As was shown in a preceeding section, the effect of the initial temperature profile appears to be slight, as long as there is at least some initial stratification. In any case, there is not enough data available to quantitatively consider this factor. The air temperature and barometric pressure probably also play a secondary role. The effect of reservoir shape will be neglected here because there is insufficient data available for reservoirs of different shapes. This could be an important effect, however.

If only the effects of size and flow rate are considered, and if Qt'_{50} is assumed to be a constant, then dimensional analysis indicates that the quantities may be related by the equation

$$Qt'_{50} = CA^{n}H_{av}^{m} \qquad (10)$$

where:

H_{av} = Average depth

n, m, C = Dimensionless numbers which may be constants

m = 3 - 2n for dimensional balance

If the average of the values of Qt'_{50} for the laboratory tests with H = 22 cm and the value of Qt'_{50} for either Field test 2, 3, or 4 are inserted in the above equation along with the pertinent geometric quantities, two equations in two unknowns, m and C, result. Solving for m and C for each of the three field tests mentioned yields:

Data Correlated	m	n	C
Field test 2 + Laboratory Tests	1.300	0.850	1.6×10^{-2}
Field Test 3 + Laboratory Tests	1.742	0.629	4×10^{-2}
Field Test 4 + Laboratory Tests	1.532	0.734	2.5×10^{-2}

Taking a numerical average of these yields:

$$\overline{C} = 2.7 \times 10^{-2}$$
$$\overline{n} = 0.75$$
$$\overline{m} = 1.5$$

$$\text{or} \quad Qt'_{50} = 2.7 \times 10^{-2} A^{0.75} H_{av}^{1.5} \qquad (11)$$

Using equation (11) to predict the laboratory and field test data yields:

Test	Qt'_{50} (predicted)	Qt'_{50} (measured)
Laboratory (H = 22 cm)	6×10^{3} cm^{3}	5.65×10^{3} cm^{3}
Field test 2	1.05×10^{10}	1.90×10^{10}
Field test 3	1.12×10^{10}	$.636 \times 10^{10}$
Field test 4	6.32×10^{9}	5.96×10^{9}
Field test 1	1.12×10^{10}	33×10^{10}

The agreement here is not very good for Field test 2 and 3, and is reasonably good for Field test 4. Since Field test 4 was performed on a lake which was the most nearly circular, it seems reasonable to assume that the introduction of a reservoir shape factor into equation (11) would reduce the error in the predicted value of Qt'_{50} for Field tests 2 and 3.

$$Qt'_{50} = DCA^{n}H^{m}_{av} \tag{12}$$

where:

D = Reservoir shape factor

The data available is not sufficient to determine what the form of the reservoir shape factor would be.

The predicted value of Qt'_{50} for Field test 1 is considerably smaller than the measured value. Since this test involved water pumping, this observation merely reinforces the conclusion reached previously (Ref. 4) that water pumping is less efficient than air injection.

VIII. CONCLUSIONS AND SUGGESTIONS FOR FURTHER STUDY

It may be concluded that a model study such as the one presented here and a scheme of analysis involving energy principles produces results which have some similarity to observed behavior in the field. However, it is difficult to determine exactly how well the model behavior reflects field behavior. Additional field testing and field test data analysis will be required before a final conclusion may be reached regarding the applicability of such a model study.

With regard to the model itself, several conclusions may be reached. First, the efficiency of the mixing process seems to be practically constant for all values of gas injection rate studied. Second, the rate of change of the per cent mixed with respect to the logarithm of time seems to be essentially constant for all laboratory (and field) tests. Third, the quantity Qt'_{50}, where Q is the gas injection rate and t'_{50} is the time at which the reservoir is 50% mixed, is approximately constant for a given reservoir geometry and initial temperature profile. If the effect of the initial temperature profile is neglected, then Qt'_{50} is strictly a function of geometry. Unfortunately, the data available was not sufficient to determine whether or not the initial temperature effects are important. Fourth, it may be concluded that the effects of radiation being received during testing may be neglected if the data is analysed in terms of per cent mixed vs. time curves. Fifth, it may be concluded that beginning gas injection before stratification has been allowed to develop is less efficient than beginning injection after the stratification has formed.

With regard to the prediction of field results on the basis of laboratory tests, it may be concluded that an analytic model based only on reservoir depth and surface area, gas injection rate, and time required for 50% mixing yields results which are accurate within an order of magnitude. Unfortunately, the results do not reflect the exact field behavior. Additional work in this area will be required to determine which additional factors (shape, initial temperature profile, etc.) need to be included in the analytic model.

In general, additional laboratory work should be performed in which the initial temperature profile and reservoir size and shape are varied. Additional field work should be performed in which the initial temperature profile and the rate of gas injection are varied for a particular reservoir. In this way, size and shape effects will be reduced and it should be possible to determine whether such laboratory features as the apparent constancy of Qt'_{50} also exist in the field.

IX. BIBLIOGRAPHY

[1] Brainard, J.P., "Induced Mixing in a Thermally Stratified Fluid," Master of Science Thesis, Massachusetts Institute of Technology, 1967.

[2] Dake, J.M.K., and D.R.F. Harleman, "An Analytical and Experimental Investigation of Thermal Stratification in Lakes and Ponds," Hydrodynamics Laboratory Report No. 99, Massachusetts Institute of Technology, September 1966, pp 157-161.

[3] Farmer, R.A., Franklin, J.P., and D.E. Wheeler, "Forced Convection in Vertically Stratified Fluids," Master of Science Thesis, Massachusetts Institute of Technology, 1961.

[4] Gay, F.T., and Z. Hagedorn, "Forced Convection in a Stratified Fluid by Air Injection," Master of Science Thesis, Massachusetts Institute of Technology, 1962.

[5] Handbook of Chemistry and Physics, The Chemical Rubber Company, 45th edition.

[6] "Bubble Gun for Destratification," Pneumatics Breakwaters Ltd., Water and Water Engineering, Vol. 65, 1961, p 7071.

[7] Irwin, W.H., Symons, J.M., and G.G. Robeck, "Impoundment Destratification by Mechanical Pumping," Journal, Sanitary Engineering Division, American Society of Civil Engineers, Vol. 92, No. SA6, December 1966, pp 21-40.

[8] Riddick, T.M., "Forced Circulation of Reservoir Water Yields Multiple Benefits at Ossining, New York," Water and Sewage Works, Vol. 104, June 1957, p 231.

[9] Symons, J.M., Irwin, W.H., and G.G. Robeck, "Impoundment Water Quality Changes Caused by Mixing," Journal, Sanitary Engineering Division, American Society of Civil Engineers, Vol. 93: SA-2:1, April 1967.

[10] Symons, J.M., Irwin, W.H., Clark, R.M., and G.G. Robeck, "Measurement and Management of D.O. in Impoundments," Journal, Sanitary Engineering Division, American Society of Civil Engineers, in press.

[11] Symons, J.M., Irwin, W.H., Robinson, E.L., and G.G. Robeck, "Impoundment Destratification for Raw Water Quality Control Using Either Mechanical- or Diffused-Air Pumping," 87th Annual Conference of the American Water Works Association, Atlantic City, New Jersey, June 4-9, 1967.

[12] Koberg, G.E. and M.E. Ford, "Elimination of Thermal Stratification in Reservoirs and the Resulting Benefits," Geological Survey Water-Supply Paper 1809-M, United States Government Printing Office, Washington, 1965.

APPENDIX A - SAMPLE CALCULATIONS

Table 5 shows a sample stability calculation for a particular time during a run. The calculation procedure was as follows:

1. Values of y and e (the voltage produced by the thermistor circuit) were taken from the output of the x - y plotter. Generally, readings were made every centimeter on the half-centimeter.

2. Values of e were converted to temperatures using the calibration charts for the ermistor.

3. Values of enthalpy per unit volume (h) and mass density (ρ) corresponding to these temperatures were taken from tables compiled from Ref. [5].

4. Δy is the increment in depth over which h and ρ were assumed to be constant (usually 1 cm, except where the temperature was uniform).

5. $\bar{y}$ is either the elevation at which the thermistor reading was made ot the mean elevation of a region of constant temperature.

6. $\bar{y}$, ρ, and Δy are multiplied together to yield the potential energy divided by g and area for the depth increment Δy.

7. The summation of $\bar{y}\rho\Delta y$ for all depth increments is the total potential energy per unit area divided by g.

8. $\Sigma h\Delta y$ is the heat content per unit area, and the summation of $\rho\Delta y$ is the mass per unit area.

9. Dividing $\Sigma h\Delta y$ by $\Sigma\rho\Delta y$ yields the average enthalpy per unit mass. This may be converted (using tables in Ref. [5]) to

the equivalent mass density (ρ_i) and temperature (T_i) for the isothermal situation.

10. $g\left[\frac{1}{2} H^2 \rho_i\right]$ is the potential energy per unit area corresponding to the isothermal state.

11. Stability per unit area is equal to $g\left[\frac{1}{2} H^2 \rho_i - \sum_{0}^{H} y \rho \Delta y\right]$.

TABLE 5. Run 3, t' = 0

y (cm)	e (mv)	T (^oC)	h (cal/cm^3)	ρ (gr/cc)	Δy (cm)	ρΔy (gr/cm^2)	$\bar{y}$ (cm)	$\bar{y}$ρΔy (gr/cm)	hΔy (cal/cm^2)
0 - 4.5	530	24.8	24.7835	.99712	5	4.98560	2.5	12.46400	123.9175
5.5	532	24.8	24.7835	.99712	1			5.48416	
6.5	533	24.9	24.8825	.99709	1			6.48413	
7.5	536	24.9	24.8825	.99709	1			7.47817	
8.5	540	25.0	24.9814	.99707	1			8.47509	
9.5	548	25.2	25.1791	.99702	1			9.47169	
10.5	560	25.5	25.4757	.99694	1			10.46787	
11.5	585	26.1	26.0687	.99678	1			11.46297	
12.5	610	26.8	26.7600	.99659	1			12.45737	
13.5	650	27.7	27.6483	.99634	1			13.45059	
14.5	695	28.8	28.7331	.99606	1			14.44243	
15.5	750	30.2	30.1123	.99561	1			15.43195	
16.5	812	32.0	31.8828	.99505	1			16.41832	
17.5	890	34.3	34.1409	.99430	1			17.40025	
18.5	958	36.3	36.1002	.99360	1			18.38160	
19.5	1025	38.4	38.1533	.99284	1			19.36038	
20.5	1055	39.4	39.1294	.99247	1			20.34563	
21.4	1060	39.5	39.2270	.99243	0.8	0.79394		16.99032	31.3816
						21.71148		236.46392	624.2251

h/ρ = 28.750923 cal/gram

T_i = 28.703 ^oC

ρ_i = 0.9960591 grams/cm^3

$\frac{1}{2}H^2\rho_i$ = 236.68356 grams/cm

-236.46392

S/gA = 0.21964 grams/cm

APPENDIX B - SOURCES OF ERROR

A. Flow Meter and Energy Input

The manufacturer states that the flow meter is accurate to within 5% of full scale reading. During operation, the meter oscillated over a range of about 5% because of the production of bubbles at the nozzle. The depth of the jet was measured with an accuracy of 1%. Therefore, the energy input calculations are accurate to within 11%.

B. Temperature Measurement and Stability Calculations

The temperature measuring apparatus is accurate to within .05^{o} C under ideal conditions. For these experiments, the accuracy was reduced by:

1. Fluid motion produced by raising and lowering the probe.
2. Time lag of the probe in adjusting to new temperatures.
3. The finite time required to take a temperature profile.
4. Variation of temperature in the radial direction not accounted for by taking measurements at only three radial locations.

The error introduced by fluid motion is difficult to determine, but its effect was not directly observable. The error introduced by thermistor response time lag was determined by measuring the difference in temperature readings for raising or lowering the probe. This difference was on the order of 0.5^{o} C. A typical value of the time rate of change of temperature was about .25 C^{o}/minute. Since the time required for taking a profile was about 2.5 minutes, an error of .6 C^{o} was thereby induced. The temperature variation between the center of the tank and the wall was about 1 C^{o}. Since measurements were made at three radii, an error of about .3 C^{o} was introduced. The maximum error in the temperature reading is, therefore, about 1.2 C^o.

In calculating stabilities, Brainard has shown that an error of 1% is introduced by taking depth increments of 1 cm, rather than integrating the curves.

APPENDIX C - LIST OF SYMBOLS

A	free surface area of tank or reservoir
a	nozzle cross-section area
B	slope of per cent mixed - log time curve
C	emperical coefficient relating Q x t'_{50} to geometry
$\bar{C}$	average of several values of C
D	reservoir shape factor
e	voltage from thermistor circuit
E_i	energy input to system
g	gravitational acceleration
h	local enthalpy
h_i	equivalent isothermal enthalpy
H	effective depth of tank or reservoir
H_{av}	average reservoir depth
H_i	equivalent isothermal tank depth
M	per cent mixed
m_a	mass of fluid in tank
m,n	emperical exponents used to relate laboratory and field data
$\bar{m},\bar{n}$	averages of several values of m and n
p	hydrostatic pressure at nozzle outlet
Q	gas volumetric flow rate at laboratory conditions
Q_1	gas volumetric flow rate at standard conditions
Q_H	heat content of body of water
S	stability
S'	stability which would have existed if water had not been artificially mixed
S_0	stability at time t' = 0

T local temperature

t time after lamps turned on

t' time after either gas injection is started or lamps are turned off (whichever comes first)

t'_o intersection of extension of linear portion of M - log t' curve with horizontal axis

t'_{50} time t' at which M = 50%

t^o time t at which $S = S_0$

V velocity of gas entering reservoir

y elevation above effective bottom of reservoir or tank

Δy increment in y (used in calculation of S)

$\bar{y}$ midpoint of y increment

z_o height of nozzle above effective bottom of reservoir or tank

γ local specific weight

γ_i equivalent isothermal specific weight

μ molecular viscosity of gas at flow meter

μ_o molecular gas viscosity at standard conditions

η efficiency of process as a function of time

η_{50} efficiency at M = 50%

ρ local mass density

ρ_n gas density at nozzle